2020

TOLL-LIKE RECEPTOR 4 INHIBITION DIFFERENTIALLY IMPACTS INTERVERTEBRAL DISC AXIAL MECHANICS IN WILD TYPE AND SPARC-NULL MICE

Mitch Whittal
whit6110@mylaurier.ca

TOLL-LIKE RECEPTOR 4 INHIBITION DIFFERENTIALLY IMPACTS INTERVERTEBRAL DISC AXIAL MECHANICS IN WILD TYPE AND SPARC-NULL MICE

by

Mitchel Connor Whittal

THESIS

Submitted to the Department of Kinesiology and Physical Education in partial fulfillment of the requirements for the degree of Master of Kinesiology

Wilfrid Laurier University

i. Abstract

Study Design. In vivo examination of the influence of TAK-242 (resatorvid) treatment on the mechanical properties of the intervertebral disc (IVD) in secreted protein acidic and rich in cysteine (SPARC) gene knockout (SPARC-null) mice.

Objectives. To examine if chronic TAK-242 treatment mitigates mechanical degradation associated with IVD degeneration in SPARC-null mice.

Summary of Background data. IVD degeneration is associated with low back pain (LBP) and is accompanied by mechanical changes to the spine. SPARC is a protein that contributes to the functioning and maintenance of the extracellular matrix (ECM), with SPARC-null mice displaying accelerated IVD degeneration. TAK-242 is a toll-like receptor 4 (TLR4) inhibitor shown to decrease proinflammatory cytokines and pain.

Methods. SPARC-null (n=29) and WT (n=26) mice aged 7-9 months were injected with TAK-242 or an equivalent volume of saline for 8 weeks (3x/per week, M-W-F). Ten spines from each group were dissected and subjected to mechanical testing. Excised lumbar spines were tested in cyclic axial tension and compression to determine neutral zone (NZ) length, NZ stiffness, compressive stiffness, tensile stiffness, and hysteresis energy.

Results. TAK-242 treatment did not impact measures of NZ stiffness ($p=0.30$) and length ($p=0.072$) despite increasing hysteresis energy ($p=0.036$), and normalized hysteresis energy ($p=0.047$). SPARC-null mice presented with smaller ($p=0.008$) and stiffer ($p=0.001$) NZs than WT mice, regardless of treatment type. Tensile stiffness was greater in SPARC-null animals

(p=0.025) but both tensile and compressive stiffness were not impacted by TAK-242 (p=0.045 and p=0.349 respectively). There was a near significant effect of mouse type on compressive stiffness; showing increased compressive stiffness in SPARC-null mice. NZ and compressive stiffness were reduced as a result of TAK-242 treatment in WT mice but not SPARC-null mice ((p=0.169 and p=0.148 respectively); suggesting a blunted effect of TAK-242 treatment in the SPARC-null model.

Conclusion. SPARC-null spines had smaller and stiffer NZs than WT mice, but TAK-242 treatment was not able to attenuate NZ changes associated with IVD degeneration in SPARC-null mice. Despite this, TAK-242 did increase hysteresis energy - indicating that hysteresis might be a more sensitive measure to detect changes to the IVD state. Reduced NZ and compressive stiffness in WT mice as a result of TAK-242 treatment indicates a blunted effect of TAK-242 in SPARC-null mice.

ii. Acknowledgements

Firstly, I would like to thank my supervisor Dr. Diane Gregory. Your guidance and expertise were crucial to the completion of this project. Your willingness to engage in animal care training alongside me was particularly appreciated.

Thank you to my lab members Josh Briar, Sabrina Sinopoli, Sara Molladavoodi for assisting with treatments, and animal care manager Kelley Putzu for guiding me through a novel experience.

To my thesis committee of Dr. Stephen Perry and Dr. Stephanie DeWitte-Orr, thank you for sharpening my thinking and improving the quality of my research. An additional thanks to Dr. DeWitte-Orr and Dr. Sarah Poynter for access to the lab space, materials, and guidance required to fulfill my thesis.

Table of Contents

iii. List of Abbreviations

ADAMTS – A disintegrin and metalloproteinase with thrombospondin motifs
AF – Annulus fibrosus
AGC – Aggrecan gene
CEP – Cartilaginous endplate
COL-2 – Type II collagen gene
DAMP – Danger/damage associated molecular patterns
DISH - Diffuse idiopathic skeletal hyperostosis
ECM – Extracellular matrix
FSU – Functional spinal unit
GAG – Glycosaminoglycans
IFN – Interferon
ILK – Integrin-linked kinase
IL-1β – Interleukin 1 beta
IVD – Intervertebral disc
LBP – Low back pain
MMP – Matrix metalloproteinases
mRNA – Messenger ribonucleic acid
NP – Nucleus pulposus
NZ – Neutral zone
PBS – Phosphate-buffered saline
RNA- Ribonucleic acid
ROM – Range of motion
SPARC – Secreted protein acidic and rich in cysteine
SPARC-null – Organism lacking the SPARC gene
TIMP – Tissue inhibitors of metalloproteinases
TLR – Toll-like receptor
TNF- α – Tumor necrosis factor alpha
uPA – Urokinase plasminogen activator
uPAR - Urokinase plasminogen activator receptor
WT – Wild-type

1. INTRODUCTION

Low back pain (LBP) currently causes more disability than any other condition globally (Hoy et al., 2014). In Canada alone, 6 – 12 billion dollars are spent on LBP-related medical costs annually (Bussières et al., 2018), with half of all Canadians experiencing a bout of LBP during a 6-month period (Vos et al., 2016). The estimated lifetime prevalence of LBP is 85% among working people (Hoy et al., 2012) resulting from a number of potential causes. LBP can arise from intervertebral disc (IVD) degeneration, disc herniations or ruptures, sprains and strains to soft tissues, radiculopathy, sciatica, spondylolisthesis, spinal stenosis, traumatic injuries, and skeletal irregularities, among other various disorders. The IVD is one of the most prominent sites of disorder, and therefore the focus in this thesis is on LBP pathology pertaining to IVD degeneration and resulting discogenic pain.

IVD degeneration has been referred to as a vicious circle that is multifactorial in nature (Vergroesen et al., 2015). A combination of altered biomechanics, heightened immune responses, and changes in gene expression, are all associated with IVD degeneration. The complex interplay between mechanics and physiology has led to the examination of potential therapeutic targets for LBP treatment and prevention. Chronic injections of TAK-242 have shown promising results in the reduction of signs of LBP in mice (Krock, Millecamps, Currie, Stone, & Haglund, 2018) but it is still unknown whether this treatment restores spine mechanics to a normal physiological state.

Additionally, examination of IVD gene expression provides detail as to how genes, and downstream protein production, are altered throughout the stages of IVD degeneration. Genes with altered expression during the course of degeneration serve as potential therapeutic targets to slow or improve the prognosis of LBP treatment.

1.1. Anatomy

1.1.1. Spinal Anatomy

The human spine articulates with the skull, ribs, and pelvis. The spine provides a partly rigid axis for rotation, allowing for maintenance of posture and movement (Moore, Agur, & Dalley, 2015). The vertebral column is composed of thirty-three vertebrae (7 cervical, 12 thoracic, 5 lumbar, 5 sacral and 4 coccygeal). Although the sacral and coccygeal regions of the spine are fused, IVDs exist between cervical, thoracic, and lumbar vertebrae of the spine for a total of 23 IVDs. Vertebrae and IVDs together form functional spinal units (FSUs) capable of motion (Figure 1).When taken in summation across entire regions of the spine, the minute contributions of FSUs allow for gross spinal movements.

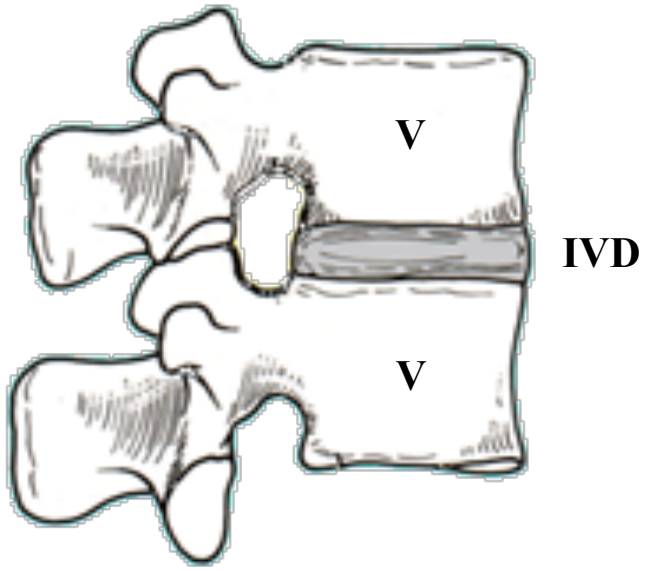

Figure 1: Lumbar functional spinal unit (FSU) composed of two lumbar vertebrae and an intervening intervertebral disc (IVD). Labels V and IVD indicate vertebrae and intervertebral disc, respectively.

1.1.2. Vertebrae

Vertebral spinous and transverse processes function as insertion sites for muscles. In conjunction with the vertebral body, transverse processes of thoracic vertebrae articulate with the ribs. Vertebral arches serve as a protective surround for the spinal cord in addition to helping protect the spinal nerves . Zygapophyseal or facet joints are articulations between adjacent vertebra composed of the superior articulating surface of one vertebra and the inferior articulating surface of another (Saravanakumar & Harvey, 2008). The opposing articular cartilage of bilateral facet joints function to guide and restrict spinal movement in addition to the transfer of loads between vertebrae (Jaumard, Welch, & Winkelstein, 2011). Vertebral size increases as you move from the cranium down to the lumbosacral region. Vertebral bodies are the main load bearing structure of the spine and thus also increase their size further down the spine to accommodate for increased load bearing. Beyond the lumbar region of the spine, vertebral size decreases from the first sacral vertebrae to the apex of the coccyx.

1.1.3. Intervertebral discs

IVDs occupy the space between adjacent vertebrae to create symphyses with vertebral bodies. In addition to permitting movement between vertebrae, the primary functions of IVDs are shock absorption and weight bearing (Khan et al., 2017), as well as the transmission of forces through the spinal column (Urban & Roberts, 2003). IVDs are composed of the nucleus pulposus (NP), annulus fibrous (AF) , and cartilaginous endplates (CEP) (Figure 2). The NP lies at the centre of the IVD and is surrounded by the AF. CEPs anchor IVDs to their surrounding vertebrae (Vergroesen et al., 2015)

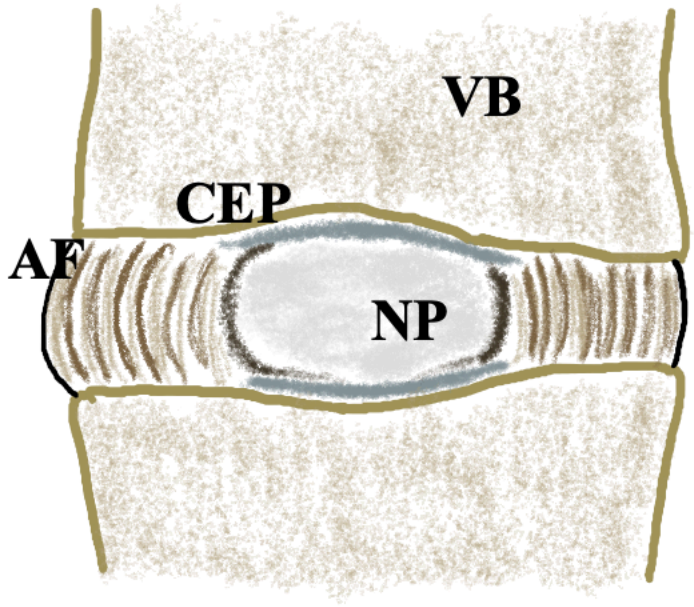

Figure 2: Intervertebral disc displaying the relative locations of the annulus fibrosus (AF), nucleus pulposus (NP), cartilaginous endplate (CEP), and vertebral bone (VB).

Nucleus Pulposus

The gelatinous NP forms the core of the IVD and provides intradiscal pressure (Vergroesen et al., 2015). A healthy NP ensures proper pressure on CEP and puts tension on the AF; contributing to disc height and the resistance of axial compressive loads (Brinckmann & Grootenboer, 1991; Hayes, Benjamin, & Ralphs, 2001; Hutton et al., 2000; Iatridis, Nicoll, Michalek, Walter, & Gupta, 2013; Inoue & Espinoza Orías, 2011; Vergroesen, van der Veen, van Royen, Kingma, & Smit, 2014).

The NP is a highly-hydrated gelatinous matrix comprised of type II collagen and proteoglycans (primarily aggrecan) (Khan et al., 2017; Urban & Roberts, 2003). Staining of sections of the bovine tail revealed that elastin fibres are oriented radially within the centre of the NP and begin to cross and overlap in the transitional region between the NP and AF (Yu, Peter, Roberts, &

Urban, 2002). Electron microscopy showed that collagen appears to be randomly organized within the NP (Inoue, 1981). The NP consists of two main cell types, chondrocyte-like cells and notochordal cells. The origin of these cells was initially unclear until it was discovered that NP cells originate solely from the embryonic notochord (Choi, Cohn, & Harfe, 2008; McCann, Tamplin, Rossant, & Seǵuin, 2012). Notochordal cells have a protective effect against NP degradation and apoptosis (Erwin, Islam, Inman, Fehlings, & Tsui, 2011) but this protective effect diminishes with age as small chondrocyte-like cells characterize the degenerated IVD (Mohanty, Pinelli, Pricop, Albert, & Dahia, 2019). Notochordal cells are of particular interest to the field of IVD regeneration research as their functions may eventually be reproduced through the reprogramming of stem cells to mimic the secretory profile of notochordal cells (Peck et al., 2017)

Annulus Fibrosus

The AF is a highly organized fibrous structure surrounding the NP that consists of approximately twenty concentric layers of type I collagen, termed lamellae (Marchand & Ahmed, 1990; Vergroesen et al., 2015). The AF functions primarily to resist transverse expansion of the IVD during axial loading (Khan et al., 2017). The AF is directly tensioned by the intradiscal pressure of the NP in response to compressive loading as well as cranial-caudal tension during the separation of the CEP (Brinckmann & Grootenboer, 1991; Iatridis et al., 2013; Inoue, 1981).

Collagen fibres run parallel to each other on an oblique angle within each lamella (Figure 3) and adjacent lamellae display approximately perpendicular fibre directions (Marchand & Ahmed, 1990; Urban & Roberts, 2003) resulting in a ply-like arrangement. Predominately water, along

with elastic fibres, type VI collagen, and proteoglycans are present in the interlamellar matrix (matrix between adjacent layers of the AF) and play a role in the maintenance of structure, the return to normal positioning after joint motion, and the binding of adjacent lamellae (Gregory, Bae, Sah, & Masuda, 2012; Urban & Roberts, 2003; Yu et al., 2002). The inner AF contains cells that are of an oval shape while the outer AF tends to be composed of longer, thin fibroblast-like cells that align with collagen fibres (Urban & Roberts, 2003).

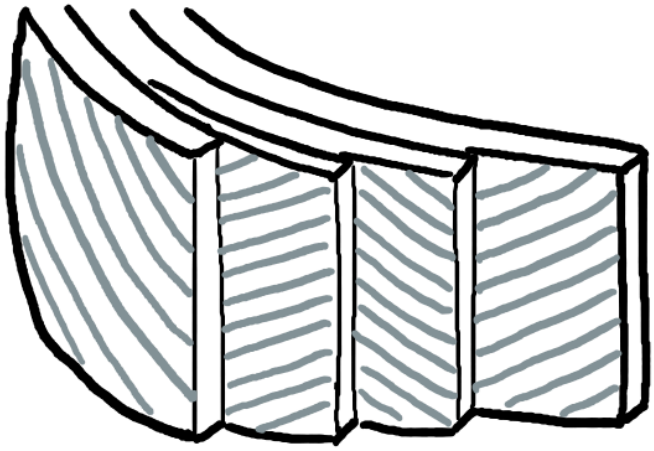

Figure 3: Depiction of the lamellae of the annulus fibrosus. Lamellae collagen fibres display a parallel relationship within each lamella and a perpendicular orientation when examining fibres of adjacent vertebrae.

Cartilaginous Endplates

CEP are composed of chondrocytes entrenched in hyaline cartilage that articulate with the lamellae of the AF at the tide-mark and the vertebral bodies at the cement line (Hayes et al., 2001; Rodrigues, Wade, Thambyah, & Broom, 2012). CEPs bind IVDs to vertebral bones and facilitate transport of nutrients between vertebral capillaries and disc cells (Lotz, Fields, & Liebenberg, 2013) as IVDs lack a dedicated blood supply. CEP fibres run horizontally – or

parallel to vertebral bodies – in a thin layer that connects into the IVD (Roberts, Menage, & Urban, 1989).

1.1.4. Inflammation and Intervertebral Disc Degeneration

IVD degeneration is a cell-mediated response (Adams & Roughley, 2006) that is characterized by the breakdown and deterioration of the ECM (Amelot & Mazel, 2018; Fraser, Osti, & Vernon-Roberts, 1993; Urban & Roberts, 2003). Proinflammatory cytokines, proteases, and neurotrophins contribute to IVD degeneration and pain. Proteases reduce proteins to amino acids, contributing the breakdown of the IVD in an inflammatory state (Alkhatib et al., 2014). Cytokines are regulatory proteins that mediate various immune and inflammatory reactions. Neurotrophins are proteins that regulate neuron development and function in addition to altering the expression of pain-related peptides (García-Cosamaló et al., 2010). Proinflammatory cytokines and neurotrophins promote innervation and sensitization (Basbaum, Bautista, Scherrer, & Julius, 2009; García-Cosamaló et al., 2010) of the normally aneural IVD (Freemont et al., 1997). This pattern has been observed in degenerated human IVDs (Edgar, 2007; Freemont et al., 1997) as well as in a mouse model of IVD degeneration (Miyagi et al., 2014). Under controlled circumstances, the inflammatory response aids in tissue healing and repair. However, when uncontrolled, the inflammatory response results in a feedforward response (Krock et al., 2018) whereby the chronic release of proinflammatory cytokines, neurotrophins, and proteases increase IVD degeneration and pain; potentially resulting in further activation of the inflammatory response.

Danger associated molecular patterns (DAMPs) are known precursors to the inflammatory response and can be initiated by many stimuli, including the endogenous detection of ECM

fragments (Schaefer, 2014). The stimuli for DAMPs, also termed alarmins (Krock et al., 2018), lead to the activation of many possible receptor families, such as toll-like receptors (TLRs), which are predominantly present in cells serving as the first line of defense in the innate immune response (Klawitter et al., 2014). Typical TLR ligands include microbial products such as metabolites or even microorganisms themselves (Takeda, Kaisho, & Akira, 2003). Once commenced, TLR activation can initiate signaling cascades that involve nuclear factor (NF)-κB, and mitogen activated protein kinases (MAPKs), leading to increased cytokine expression (Klawitter et al., 2014). NF-κB activation initiates a pathway with both proinflammatory and anti-inflammatory effects (Lawrence, 2009). MAPK pathways allow TLRs to regulate inflammatory and catabolic responses upon ligand binding (Quero et al., 2013). Confirmation of these pathways leading to IVD degeneration came in the form of lipopolysaccharide (LPS) induced TLR4 activation in rats. In vitro and in vivo LPS stimulation resulted in increased cytokine levels in addition to the intradiscal injections of LPS causing moderate IVD degeneration (Rajan et al., 2013).

1.1.5. Anatomical Changes with Intervertebral Disc Degeneration

Notable changes that characterize IVD degeneration include decreased IVD height, in-growth of nerves and blood vessels into the IVD, herniation, CEP calcification, decreased IVD cells, and increased variability in annular collagen fibril size (Gruber et al., 2005; Vincent et al., 2019). During growth and maturation, the distinction between the NP and AF diminishes as proteoglycan synthesis decreases and collagen synthesis increases (Khan et al., 2017). As such, the age-dependent morphological changes that follow are a less gelatinous – and more fibrous – NP, with the IVD decreasing in its overall level of organization (Buckwalter, 1995; Urban &

Roberts, 2003). Although normally avascular and mostly aneural, degenerated IVDs display increased vascularization and innervation due to altered tissue integrity and the presence of elevated cytokines and neurotrophins (Basbaum et al., 2009; Edgar, 2007; Raj, 2008).

During degeneration, IVD proteoglycan content degrades reducing hydration with greater reductions in the NP than the AF (Khan et al., 2017; Roughley, Melching, Heathfield, Pearce, & Mort, 2006). Reduced hydration causes intradiscal pressure to drop, leading to the loss of IVD height (Brinckmann & Grootenboer, 1991; Sato, Kikuchi, & Yonezawa, 1999; Vergroesen et al., 2014), which in turn results in increased radial bulging due to reduced lamellar tension (Brinckmann & Grootenboer, 1991). Also with age and degeneration, lamellae become divided with irregular overlapping of AF fibres as the collagen and elastin become disorganized (Urban & Roberts, 2003). Potential CEP changes include sclerosis of the vertebral subchondral bone and damage in the form of lesions (Rutges et al., 2011; Wang, Videman, & Battié, 2012).

1.2. Intervertebral Disc Biomechanics

1.2.1 The Neutral Zone

The measurement of force is key to quantifying the mechanical properties of spinal motion. Utilization of force-displacement data allows for the quantification of the neutral zone (NZ). The NZ is a linear region of low resistance to motion (Figure 4) (Gsell, Zwambag, Fournier, Séguin, & Brown, 2017; Panjabi, 1992; Smit, van Tunen, van der Veen, Kingma, & van Dieën, 2011). NZ properties have shown greater sensitivity than range of motion (ROM) properties in their ability to detect changes in spinal stability (Hasegewa, Kitahara, Hara, Takano, & Shimoda, 2009; Panjabi, 2003). NZ stiffness in particular, is a commonly utilized variable when examining

spinal stability. Stiffness is a measure of the extent to which an object or material resists displacement in response to force. Practically, NZ stiffness is calculated as the slope of the NZ on a force-displacement curve (Cannella et al., 2008; Elliott & Sarver, 2004; Gsell et al., 2017; Johannessen, Cloyd, O'Connell, Vresilovic, & Elliott, 2006; Sarver & Elliott, 2005), and is often averaged between compression and tension curves in axial loading. NZ properties are typically examined during flexion-extension but can also accurately depict spinal stability properties during tension-compression (Cannella et al., 2008; Elliott & Sarver, 2004; Gsell et al., 2017; Johannessen et al., 2006; Sarver & Elliott, 2005). NZ length is also often calculated to provide an indication of the amount of spinal motion of an FSU. NZ length is simply the difference in displacement between the endpoints of the NZ. A stiffer and shorter neutral zone indicates that a tissue is deforming very little in response to an applied force in its region of minimal resistance to motion and that this region of low resistance exists for less total displacement.

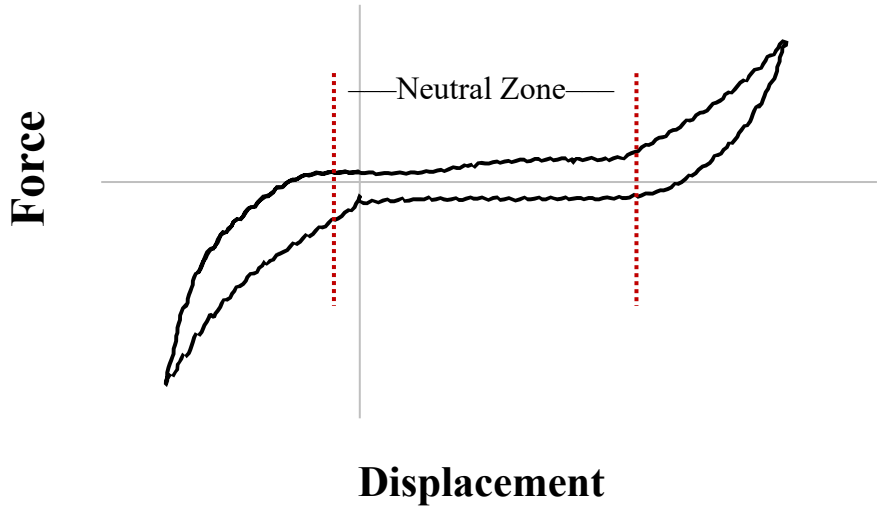

Figure 4: Force-displacement graph generated from axial loading of a mouse lumbar spine. Approximate NZ is identified in red.

1.2.2. Axial Loading

Stabilization of the spinal column is attributed to muscle forces as well as motion segment stiffness (Gardner-Morse & Stokes, 2003). The spinal column must function to endure mostly compressive loading while still allowing for mobility. The anterior column is responsible for majority of the load transmission between vertebrae with the posterior facets supporting less than twenty percent of the load in each segment (Nachemson, 1960). Within the motion segment, the NP acts as a semi-fluid fulcrum for FSUs, allowing movement in six degrees of freedom (Moore et al., 2015). Under axial compression, the NP becomes pressurized and undergoes axial and radial displacements that are resisted by the AF (Fan, Ghista, Sridhar, & Ramakrishna, 2005). The AF is hence stiffened under loading; effectively bearing heavy loads without collapsing or radially herniating under normal circumstances (Fan et al., 2005). The inner AF resists deformation of the NP but also behaves like the pressurized NP in the resistance to compression, while the outer AF functions more like a tensile wrap around the IVD (Adams, Mcnally, Dolan, & Mcnally, 1996). The presence of intradiscal pressure is crucial for proper tensioning of the AF, translation of pressure to CEP, and maintenance of segment stiffness in axial compression (Brinckmann & Grootenboer, 1991; Brown, Gregory, & McGill, 2008; Vergroesen et al., 2015; Vergroesen et al., 2014). Pressurization of the NP is essential to the maintenance of IVD mechanical properties in addition to interlamellar shear resistance of AF layers (Adam, Rouch, & Skalli, 2015; Cannella et al., 2008). Comparison of old and young (4-5 months vs 20-22 months) mice found no difference in compressive stiffness despite differences in tensile properties (Holguin, Aguilar, Harland, Bomar, & Silva, 2014).

IVDs undergo compression and tension simultaneously at opposing sides of the IVD when moving through flexion, extension, and lateral bending (Moore et al., 2015). As such, it is important to understand the potential consequences to the IVD when subjected to both compression and tension. Tensile stiffness of the IVD is mainly derived from the strength of lamella and the adhesion between annular lamellae. Examining the tensile properties of the AF reveals that it behaves in an anisotropic manner such that the orientation of an excised AF sample (radial, circumferential, or axial) impacts its behaviour when placed into tensile loading (O'Connell, Guerin, & Elliott, 2009). In the axial testing of excised AF samples, radial samples were 2.7x stiffer in their toe-region as a result of degeneration while axial and circumferential samples did not differ mechanically between degenerated and non-degenerated samples (O'Connell et al., 2009). Cyclic tensile loading of degenerated and non-degenerated human circumferential-axial AF samples determined that degenerated AF samples were stiffer – as indicated by greater dynamic modulus (Sen, Jacobs, Boxberger, & Elliott, 2012). This is in contrast to quasistatic testing methods that found no differences in AF tensile modulus with degeneration (Acaroglu et al., 1995). At the IVD level, tensile stiffness decreased in the lumbar region of old mice in comparison to young mice (4-5 months vs 20-22 months) but increased in the coccygeal region from young to old (Holguin et al., 2014). When stretched until failure, the hyaline cartilage connecting IVDs to the subchondral bone of vertebrae was found to be the weakest region in 10/14 specimens (Balkovec, Adams, Dolan, & Mcgill, 2015), while the remaining specimens saw damage to the AF in the form of tearing and delamination (2/14), or trabecular bone fracture (2/14); highlighting the great tensile strength of the IVD.

1.2.3 Biomechanical Changes to the Intervertebral Disc with Degeneration

At the onset of degeneration, proteoglycan concentration in the NP decreases while collagen content increases, resulting in an overall loss in hydration. Accompanying these molecular changes are altered mechanics of the IVD. Initially, spine stiffness decreases as the IVD becomes unstable (Hasegewa et al., 2009; Inoue & Espinoza Orías, 2011; Mimura et al., 1994). Later and more severe stages of IVD degeneration result in increased spinal stiffness, beyond what is considered physiologically normal (Fujiwara et al., 2000; Gsell et al., 2017; Manohar Panjabi, 2003). Modelling for DISH (diffuse idiopathic skeletal hyperostosis), equilibrative nucleoside transporter 1 (ENT1) deficient mice develop progressive ectopic calcification of spinal connective tissues and display increased spinal stiffness. Additionally, paraspinal passive muscle stiffness was found to remodel in response to the spine stiffness (Gsell et al., 2017). This observed compensatory relationship between spine stiffness and passive muscle stiffness supports the hypothesis by Panjabi et al. 2003 stating that the spinal stabilizing system strives to return spinal properties to normal through compensatory stiffening of the spinal column or altered muscle activation.

The NP decreases in its load bearing capacity as it loses hydrostatic pressure (Inoue & Espinoza Orías, 2011). With a loss of hydrostatic pressure, the stress distribution of the IVD becomes anisotropic with pressure concentrations in the AF as opposed to the equal, isotropic distribution of a healthy IVD (McNally & Adams, 1992). Finite element modelling manipulating reductions in intradiscal pressure led to decreased axial forces transmitted through the IVD (Shirazi-Adl, 1992; Shirazi-Adl, Ahmed, & Shrivastava, 1986). With the noted decrease in load bearing capacity of the NP, the AF and posterior elements – such as facet joints – see an increase in

transferred load during compression loading (Niosi & Oxland, 2004; Yang & King, 1984). Despite these changes, there does not seem to be a significant loss in the tensile strength of the AF (Ebara et al., 1996).

1.2.4 Hysteresis

Hysteresis is a viscoelastic property of biological tissues that occurs with repetitive loading of the IVD (Kazarian, 1975). Hysteresis calculations are used to quantify energy absorption of IVDs (Chow, Luk, Holmes, Li, & Tam, 2004). For IVD mechanics, hysteresis energy is quantified by measuring the area between the tensile and compressive curves on a force-displacement graph (Figure 5). Energy absorption of the IVD typically decreases throughout the degenerative process (Lundon, Bolton, Diploma, & Physiotherapyz, 2001; Nuckley et al., 2008).

Human cadaveric research examined hysteresis energy in axial rotation (AR), lateral bending (LB), and flexion-extension (FE) across varying degrees of IVD degeneration (Muriuki et al., 2016; Zirbel, Stolworthy, Howell, & Bowden, 2013). The effects of degeneration on hysteresis energy is still unclear as Zirbel et al. 2013 demonstrated an increase in AR hysteresis, a decrease in LB hysteresis, and no statistical change for FE hysteresis. Muriuki et al. 2016 reported no effect of degeneration on FE or AR hysteresis and an increase in LB hysteresis with degeneration. Despite this, both studies found significantly different hysteresis between segmental levels of the lumbar spine in AR and LB. Zirbel et al. 2013 noted decreased AR hysteresis and increased LB hysteresis between upper and midlumbar segments. Muriuki et al. 2016 also reported decreased AR hysteresis in the midlumbar region but LB hysteresis was greatest for the upper lumbar segments as opposed to midlumbar segments.

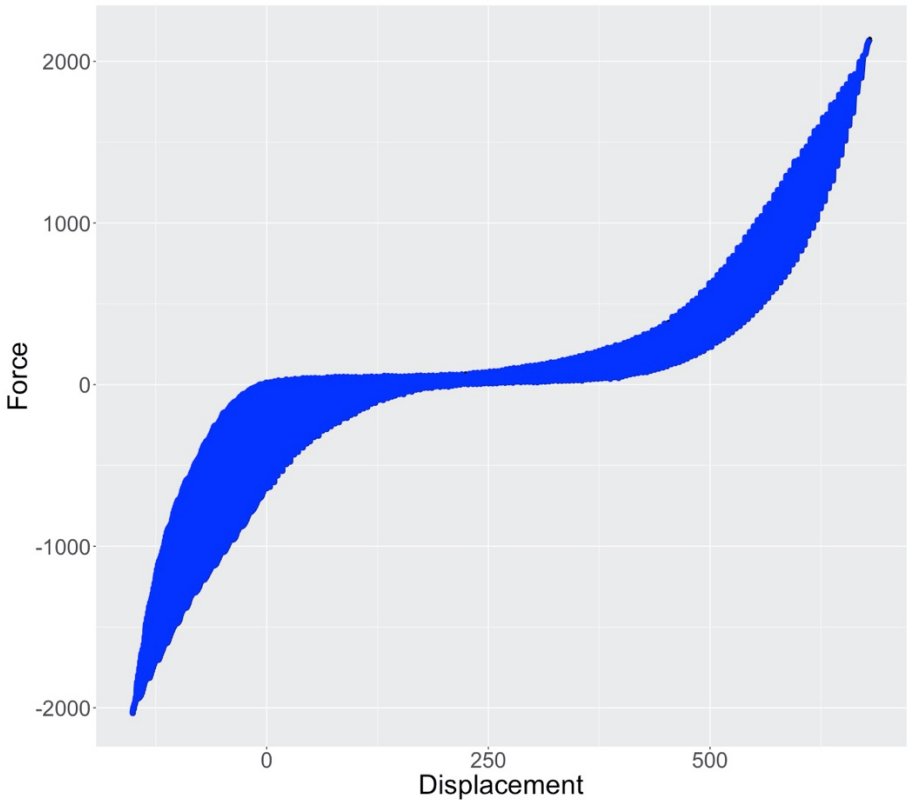

Figure 5: Force-displacement curve with area between the tension and compression curves coloured in blue. This area represents hysteresis energy.

1.3. Secreted Protein Acidic and Rich in Cysteine (SPARC)

Secreted protein acidic and rich in cysteine (SPARC) or osteonectin is a matricellular protein residing in the extracellular matrix. Matricellular proteins alter cell function through interactions with cell surface receptors, hormones, proteases, structural proteins like collagen, and other molecules (Bornstein, 2009). SPARC has a role in the mineralization of bone and cartilage due to its affinity for type I collagen, hydroxyapatite, and calcium (Metsäranta, Young, Sandberg, Termine, & Vuorio, 1989; Pacifici, Oshima, Fisher, Young, Shapiro, 1990; Termine et al., 1981). Further, SPARC functions to remodel the ECM in response to injury (Bornstein & Sage, 2002; A D Bradshaw & Sage, 2001; Sweetwyne et al., 2004) by interacting with proteins at the surface of cells to enable changes in structure and shape (Sage & Bornstein, 1991).

SPARC functions to remodel the ECM, and IVD degeneration is commonly characterized by ECM breakdown (Amelot & Mazel, 2018). As such, it is logical that a mouse model lacking the SPARC gene (SPARC-null) has been validated as a mechanical model for IVD degeneration (Elliott & Sarver, 2004). Within the IVD itself, SPARC is expressed to a greater degree in the outer AF than the inner AF and the NP (Gruber, Ingram, Leslie, & Hanley, 2004). Expression of SPARC decreases with age and degeneration (Gruber et al., 2004) with the SPARC-null mouse displaying increased proinflammatory cytokines (Krock et al., 2018), increased innervation of IVDs , and accelerated IVD degeneration (Gruber et al., 2005). SPARC gene knockout results in increased collagen surface receptor interactions, and hence reduced control over collagen fibril formation and procollagen maturation (Bradshaw, 2009). SPARC-null fibroblasts also have a reduced ability to fashion fibronectin into fibrils in addition to altered fibronectin- ILK (integrin linked kinases) that results in lower ILK cell-contractile signalling (Barker et al., 2005). IVD degeneration in SPARC-null mice was confirmed through changes in disc height index (Krock et al., 2018) in addition to histological and x-ray image analysis showing wedging and a loss of negatively charged proteoglycans (Gruber et al., 2005). SPARC-null mouse IVDs had negatively affected: numbers of IVD cells, collagen fibrils, type I collagen content, as well as structural changes in the form of wedging, herniations, and CEP calcification (Gruber et al., 2005). Histological examination of WT and SPARC-null IVDs and found dorsal herniations in SPARC-null IVDs of mice aged 14,19, and 20 months (Gruber et al., 2005). Herniations were only present in SPARC-null IVDs and were also distinguished by a reduction of proteoglycan content, which decreases disc hydration and hampers the shock absorber capabilities of the disc (Gruber et al., 2005). Mechanically, SPARC-null mice were found to have increased NZ stiffness and

decreased NZ length (Whittal et al., 2020) compared to wildtype. Behaviourally, SPARC-null mice display elevated axial and radiating pain (Krock et al., 2018; Millecamps, Czerminski, Mathieu, & Stone, 2015; Millecamps, Tajerian, Sage, & Stone, 2011) in addition to motor impairments and hypersensitivity to cold (Millecamps et al., 2015; Millecamps, Tajerian, Naso, Sage, & Stone, 2012).

1.4. TLR4 Signalling and TAK-242 (Resatorvid)

TLRs 1, 2, 4 and 6 have shown increased activation with IVD degeneration in humans (Klawitter et al., 2014). TLR2 activation has shown to increase inflammatory cytokine expression, proteases, and neurotrophins in cultured human IVD cells (Klawitter et al., 2014; Krock et al., 2016; Quero et al., 2013). TLR4 is activated through the binding of DAMPs (damage associated molecular patterns), or alarmins (Krock et al., 2018). In the case of IVD degeneration, TLR4 may bind fragmented ECM fibrous proteins such as fibronectin or aggrecan. Once activated, TLR4 initiates cellular signalling via 2 pathways (Vaure & Liu, 2014). The first, and most prominent is the TIRAP–MyD88 pathway that controls early NF-κB activation and leads to the synthesis of cytokines. NF-κB promotes the M1 macrophage phenotype and induces the expression of proinflammatory genes, leading to the synthesis and release of cytokines and chemokines by macrophages (Liu, Zhang, Joo, & Sun, 2017). The second, and less prominent pathway is the TRIF–TRAM pathway that activates IRF_3 – interferon regulatory factor-3 and upregulates type 1 interferons (IFNs) (Nilsen et al., 2015; Vaure & Liu, 2014; Verstak et al., 2014). IFNs and IRF_3 function to protect surrounding cells from infection by stimulating cells to produce proteins that prevent viruses from replicating within cells. The TRIF–TRAM pathway also stimulates TNF-α production and secretion, which leads to the activation of NF-κB later in

its signalling cascade than the TIRAP–MyD88 pathway once TNF-α binds to its receptor (Vaure & Liu, 2014). Also downstream to TLR4 signalling is MAPK activation (Li et al., 2015; Nyati et al., 2017). MAPK phosphorylates a variety of substrates and regulates the expression of many cytokines (De Souza et al., 2014).

TAK-242 is a cyclohexene derivative (Ii et al., 2006) that selectively binds and inhibits TLR4, a transmembrane protein that many DAMPs bind to in commencing the innate immune response (Kuzmich et al., 2017). TAK-242 inhibits TLR4 through selectively binding to its intracellular domain at the Cys747 site (Takashima et al., 2009). It is hypothesized that the configuration of amino acids at 747 is vital to TLR4 signalling and that TAK-242 is recognized by the cysteine residues of site 747. Binding of TAK-242 is believed to alter the environment around Cys747; changing the intracellular domain to an inactive conformation through covalent bonding (Takashima et al., 2009). disrupting its protein-protein interactions with adaptors TIRAP and TRAM (Matsunaga, Tsuchimori, Matsumoto, & Ii, 2011). This disruption inhibits phosphorylation of MAPKs, TIRAP mediated activation of NF-κB, TRAM regulated activation of NF-κB and IFNs, as well as the subsequent resulting inflammatory response that occurs with TLR4 activation (Takashima et al., 2009). TAK-242 treatment suppresses cytokine production (Ii et al., 2006; Krock et al., 2018; Matsunaga et al., 2011) and has been examined for its efficacy to reduce measures of LBP in SPARC-null mice (Krock et al., 2018). Chronic TLR4 inhibition via TAK-242 treatment led to decreased behavioural signs of LBP, reduced IVD inflammation and pain-related neuroplasticity (Krock et al., 2018).

1.6. Use of Mouse Spines to Model Human Lumbar Intervertebral Discs

The use of experimental animals is necessary to allow for the use of genetically engineered models of degeneration like the SPARC-null mouse. In contrast to the thirty-three vertebrae of the human vertebral column, C57BL/6N or "black 6" mice have a vertebral column made up of fifty-nine to sixty-one vertebrae (Shinohara, 1999). Human and black 6 mice have the same number of cervical vertebrae, but the rodent vertebral column contains an additional thoracic (13) and lumbar (6) vertebrae, contrasted by one fewer (4) sacral vertebrae. The coccygeal region, composed of twenty-nine to thirty-three vertebrae creates the rodent tail (Shinohara, 1999). A main concern when employing the quadruped rodent as a mechanical model for human lumbar spines is the horizontal position of rodent spines. Despite the obvious difference between bipedal humans and quadruped rodents, both spine orientations experience their primary loading along their long axes (Smit, 2002). In quadruped animals, compressive spine forces are generated by tensile forces of muscles during walking (Smit, 2002), and may account for the increased vertebral bone density in some quadruped species (Hauerstock, Reindl, & Steffen, 2001). Mechanically, mouse and rat IVDs have been validated as mechanical models for human lumbar discs. When normalized for disc height and area, rat and mouse IVDs had mechanical properties representative of human lumbar spines in axial loading as well as torsion (Elliott & Sarver, 2004). Further, analyses showed that mechanical properties across quadruped species were very similar when normalized for geometry (Beckstein et al., 2008). Mice utilized in the current experiment began treatment with mean ages ranging from 8-9 months (Figure 6). By the end of treatment injections, mice were 10-11 months old, placing them in the middle-aged category of mice; comparable to a human in their late 30's (Fox et al., 2007). Mice are considered mature after 3-6 months, middle aged from 10-14 months, and old from 18-24 months (Fox et al., 2007).

2. PURPOSE AND HYPOTHESES

Chronic injections of TAK-242 have shown promising results in the reduction of signs of LBP in mice (Krock et al., 2018), yet much still remains unknown. The purpose of this study was to examine the effects of chronic TAK-242 treatment on the mechanical properties of the IVD in uniaxial loading in SPARC-null and WT mice.

Hypotheses

1. TAK-242 treatment was expected to mitigate mechanical changes of IVD degeneration; as such, the combination of SPARC-null mice and TAK-242 treatments was predicted to display similar NZ properties to Wild-type (WT) mice injected with saline and WT mice injected with TAK-242. SPARC-null mice treated with saline injections were hypothesized to have smaller and stiffer NZs than the other three treatment groups.
2. Tensile stiffness was expected to be greater in SPARC-null mice and TAK-242 was predicted to reduce tensile stiffness. Compressive stiffness was expected to be similar between treatments and mouse types as previous research indicated no change in compressive stiffness between healthy and degenerated lumbar IVDs (Holguin et al., 2014).
3. As hysteresis energy typically decreases with degeneration (Lundon et al., 2001; Nuckley et al., 2008), it was expected that mice treated with TAK-242 would display greater hysteresis energy than mice injected with saline. Additionally, SPARC-null mice were predicted to show less hysteresis energy than WT mice due to their accelerated IVD degeneration.

3. METHODS

3.1. Experimental Animals

Fifty-five (26 WT and 29 SPARC-null) C57BL/6N ("black 6") mice aged 7-9 months were examined. Experimental animals were quasi-randomized to ensure no significant differences in age and initial mass (Figure 6) . The four conditions include: 1. SPARC-null mice with TAK-242 injection (14 mice), 2. SPARC-null mice with saline (vehicle) injection (15 mice), 3. Wild-type (WT) mice with TAK-242 injection (14 mice), and 4. WT mice with saline (vehicle) injection (12 mice). Ten animals per group were mechanically tested (n=40) and the remaining animals in each condition were utilized for gene expression analysis (n = 15). Sample size was based on previous research that investigated the effects of TAK-242 treatment on behavioural and inflammatory changes in mice (Krock et al., 2018).

CONDITION	AGE (months)	MASS (g)
WT Vehicle	8.37 (0.66)	33.78 (7.52)
WT TAK-242	8.49 (0.61)	33.64 (7.0)
SPARC-null Vehicle	8.75 (0.98)	30.73 (4.16)
SPARC-null TAK-242	8.71 (1.06)	30.43 (3.39)

Figure 6: Mean (standard deviation) age and mass of mice at the onset of treatment.

3.1.1. Animal Care and Treatment

SPARC-null and WT mice were randomly assigned to either TAK-242 injections or sham protocol. TAK-242 (10 mg/kg, 1 mg/ml in saline with 5% dimethyl sulfoxide (DMSO) and 5% Tween 80) or an equivalent volume of phosphate buffered saline (PBS) was injected through *i.p.*

injections with manual restraint 3 times per week (M-W-F; same time of day for each injection) for 8 weeks as per the outlined directions in SOP C31 – "Intraperitoneal Injection in the Rodent". Schedule and dosage were determined from previous studies (Krock et al., 2018; Woller et al., 2016; Zhao, Xin, Gao, Teng, & Chu, 2015). After injections, animals were monitored according to SOP C13 – " Treatment and Monitor log", including daily monitoring when animals were stable. Mice were housed in groups of 2-4 animals and provided with Carefresh bedding and typical enrichment. Following 8 weeks of injections, mice were anesthetized with isoflurane and euthanized via carbon dioxide in accordance to the guidelines in SOP E1 – "Euthanasia" and SOP E2.

3.1.2. Dissection and Preparation

Whole mice were thawed at 4°C overnight for a minimum of 16 hours. Spines were excised and immersed in a phosphate buffer solution (PBS) for 20 minutes prior to full dissection. Spines were then dissected to the osteoligamentous level (Figure 7) and the lumbar portion of each spine was excised for mechanical testing.

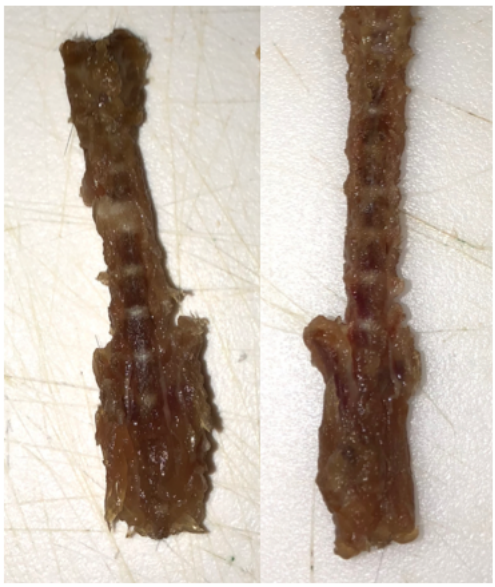

Figure 7: Dissected osteoligamentous mouse spines with only the remaining IVD, vertebrae and ligamentous tissue.

3.2. Mechanical Testing Protocols

Intact spines from L2/3 to L4/5 were tested in cyclic uniaxial tension and compression at a rate of 0.33% displacement/second, with force and displacement data sampled at 30 Hz (Gsell et al., 2017). Lumbar spines were clamped and mounted (Figure 8) in a mechanical testing system (BioTester, CellScale Biomaterials Testing, Waterloo, Canada). Displacement-controlled limits testing of each spine determined the appropriate tensile and compressive displacements as to not exceed the limits of a 2.5N load cell. Once the displacement limits were determined, a cyclic test of 15 cycles was completed and the force-displacement data of the 15th cycle used for analysis (Gsell et al., 2017). This process was repeated with three (L2/3-L4/5), two (L3/4-L4/5), and one (L4/5) IVDs tested in series, for a total of three tests per spine. Previous research demonstrated that 10-15 cycles are sufficient to produce consistent loading curves and mitigate potential effects of superhydration (Elliott & Sarver, 2004; Johannessen et al., 2006).

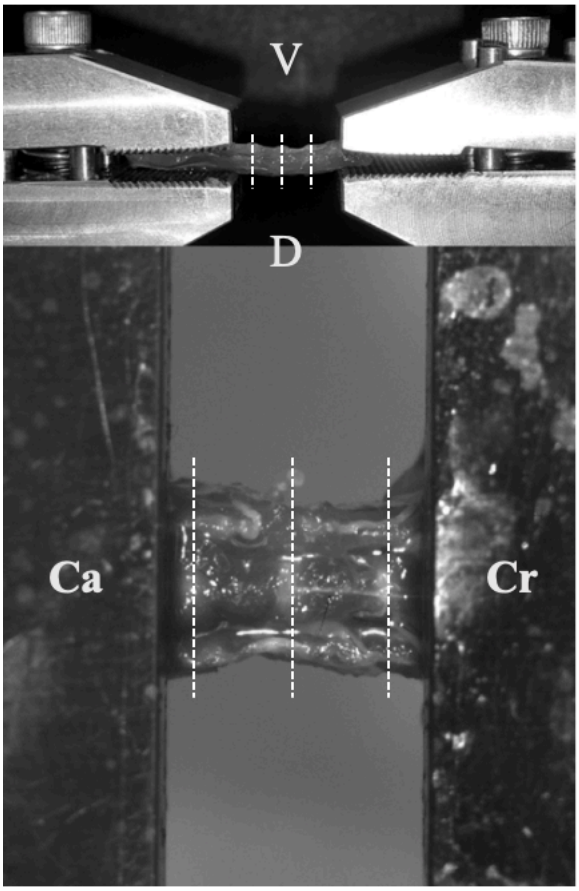

Figure 8: Top view of excised and mounted L2/3, L3/4, and L4/5 segments of the lumbar spine. White dotted lines indicate the three IVD levels. V, D, Ca, and Cr indicate ventral, dorsal, caudal, and cranial.

3.3. Data Analysis

Force data was sampled at 30Hz using the mechanical testing system (BioTester, CellScale Biomaterials Testing, Waterloo, Canada). Mechanical NZ properties were reported from axial loading in tension and compression. Previous research indicated that NZ properties during axial loading are also likely representative of NZ properties in bending (Cannella et al., 2008; Elliott & Sarver, 2004; Gsell et al., 2017; Johannessen et al., 2006; Sarver & Elliott, 2005). NZs were independently and blindly identified visually (Figure 9) and averaged in both tension (top of force-displacement curve) and compression (bottom of force-displacement curve) (Whittal et al.,

2020). Compressive and tensile stiffness calculations were used to quantify mechanical responses of IVDs outside of their NZs. Compressive stiffness was calculated as the slope of the force-displacement region highlighted in blue (Figure 9). Tensile stiffness was calculated as the slope of the force-displacement curve identified in green (Figure 9). Hysteresis energy was calculated as the area between tensile (upper) and compressive (lower) curves on force-displacement data using the polyarea() function in R (version 3.6.2). All force-displacement traces followed a similar double sigmoid shape with identifiable tensile and compressive toe regions separated by a neutral zone. Hysteresis energy was then normalized to the ROM of each test to account for differences in reached displacements. Normalization was conducted by dividing hysteresis energy results by the absolute value of summed displacement of each test in tension and compression.

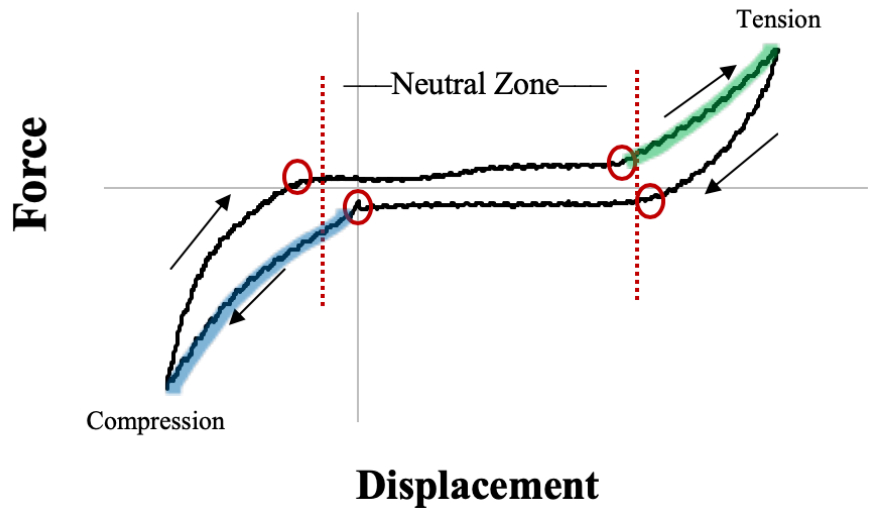

Figure 9: Representative trace of a force-displacement curve. Red circles indicate neutral zone endpoints in both tension (top curve) and compression (bottom curve). Displacement between points and corresponding slope of the force-displacement tracing for each curve (tension and compression) were calculated (R>0.95) and averaged to quantify the NZ size and stiffness.

3.4. Statistical Analysis

A linear mixed effects model fit by maximum likelihood was conducted to determine the effects of mouse type (WT vs SPARC-null), treatment (TAK-242 vs vehicle), and the number of IVDs tested in series (one vs two vs three) on NZ length, NZ stiffness, tensile stiffness, compressive stiffness, and hysteresis. Number of IVDs tested in series, or level, was included as a random effect to account for repeated measures. Given that the number of discs tested in series was the greatest predictor of hysteresis energy – with more discs producing greater hysteresis energy, normalized hysteresis was calculated to account for the differences in reached displacements between tests performed with different numbers of IVDs tested in series. Normalized hysteresis data was then pooled across testing levels and evaluated with a factorial ANOVA that utilized mouse type and treatment as independent variables. Individual ANOVAs were also performed on WT and SPARC-null animals independently for the measures of NZ stiffness, NZ length, tensile stiffness and compressive stiffness. A significance level of $\alpha = 0.05$ was employed for all statistical tests. All reported descriptive statistics are stated as mean (standard deviation). All statistical tests were performed using R (version 3.6.2) open source software and executed in RStudio (version 1.2.5033).

4. RESULTS

4.1 NZ Stiffness

Collapsed across treatment conditions, NZ stiffness was significantly greater in SPARC-null mice compared to WT (p=0.001), SPARC-null: 1.81 mN/µm (1.06), WT: 1.43 mN/µm (0.80). There was no main effect of treatment on NZ stiffness (p=0.30). A near significant interaction between mouse type and treatment was found (p=0.057). Independent analysis of each mouse type revealed a main effect of TAK-242 in WT mice (p=0.032), and not WT mice (p=0.412).

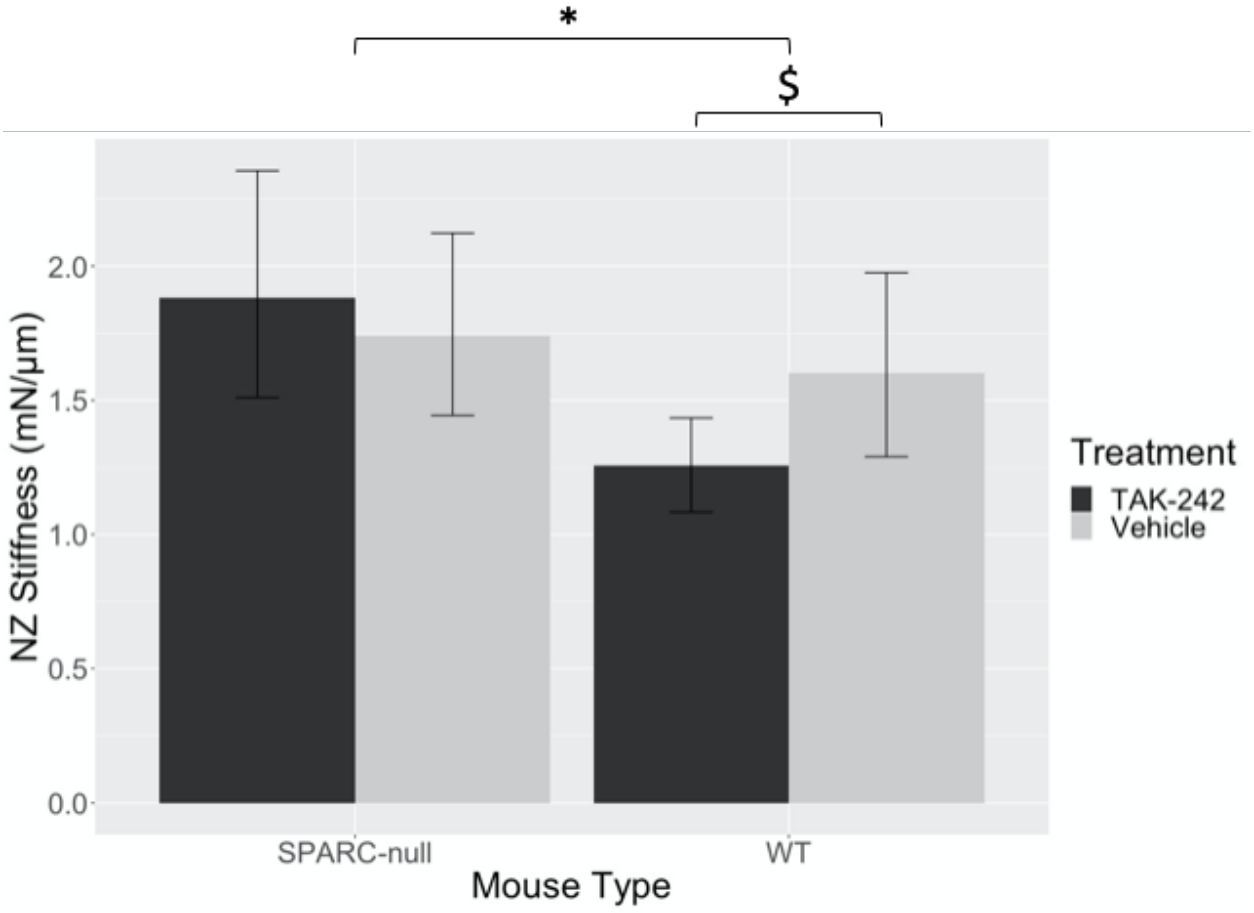

Figure 10: Mean NZ stiffness (mN/µm) of SPARC-null and WT groups collapsed across mechanical tests performed with 1,2, and 3 IVDs tested in series. Error bars depict standard deviation. * denotes statistical significance independent of mouse type. $ denotes statistical significance in WT mice only. A total of 40 spines were tested with n=10 per group, for a total of 120 included tests.

4.2 Tensile Stiffness

Tensile stiffness was significantly greater in SPARC-null mice compared to WT (p=0.025) with mean values of 5.99 mN/μm (1.04) and 5.65 mN/μm (1.50) for SPARC-null and WT mice. There was no effect of TAK-242 treatment on tensile stiffness across mouse types (p=0.45) as well as within WT (p=0.148) and SPARC-null mice (p=0.417). There was no found mouse type – treatment interaction, p=0.093.

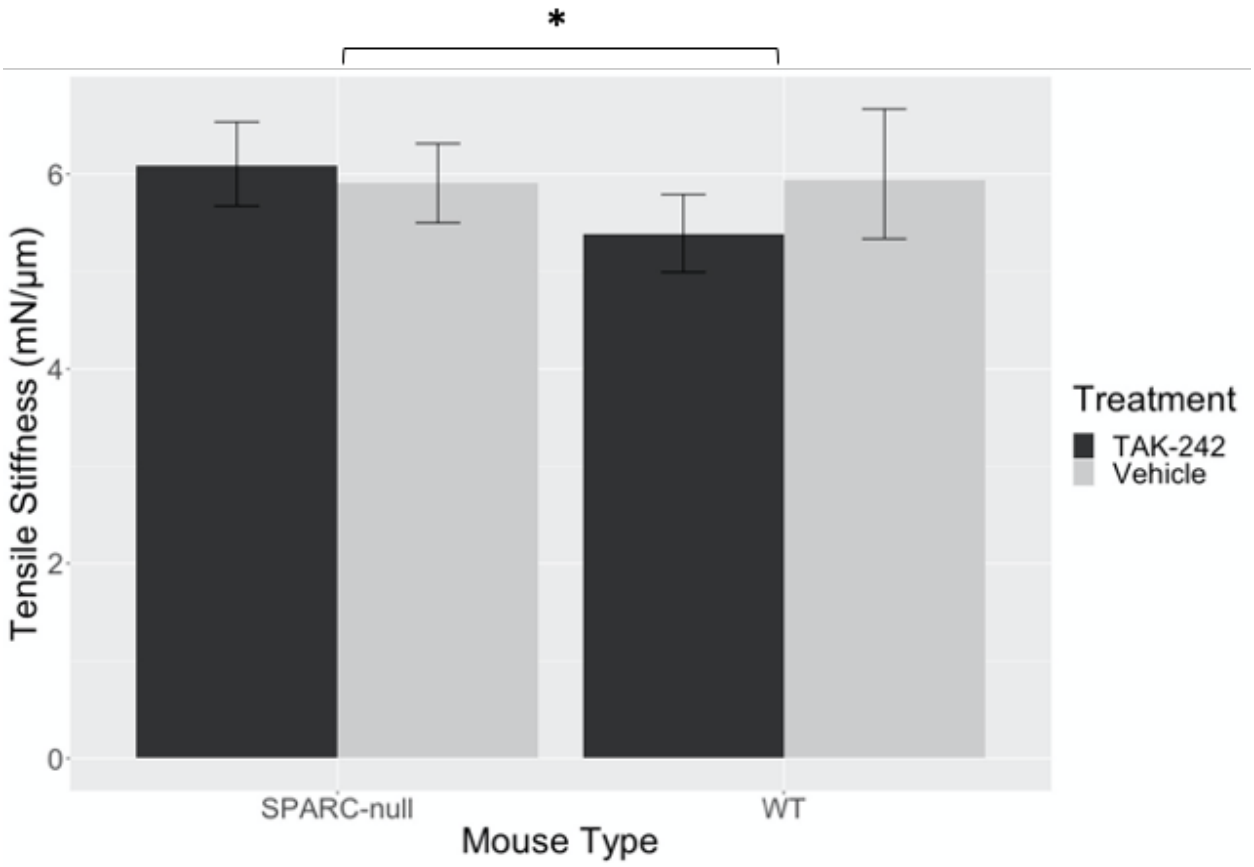

Figure 11: Mean tensile stiffness (mN/μm) of SPARC-null and WT groups collapsed across mechanical tests performed with 1,2, and 3 IVDs tested in series. Error bars depict standard deviation. * denotes statistical significance. A total of 40 spines were tested with n=10 per group, for a total of 120 included tests.

4.3 Compressive Stiffness

There was a near significant effect of mouse type on compressive stiffness (p=0.059, SPARC-null: 8.88 mN/μm (2.48), WT: 8.46 mN/μm (2.20)), and no effect of treatment group (p=0.349). There was also no interaction between mouse type and treatment (p=0.120). A main effect of TAK-242 treatment was present in WT mice (p<0.001), but not SPARC-null mice (p=0.3919).

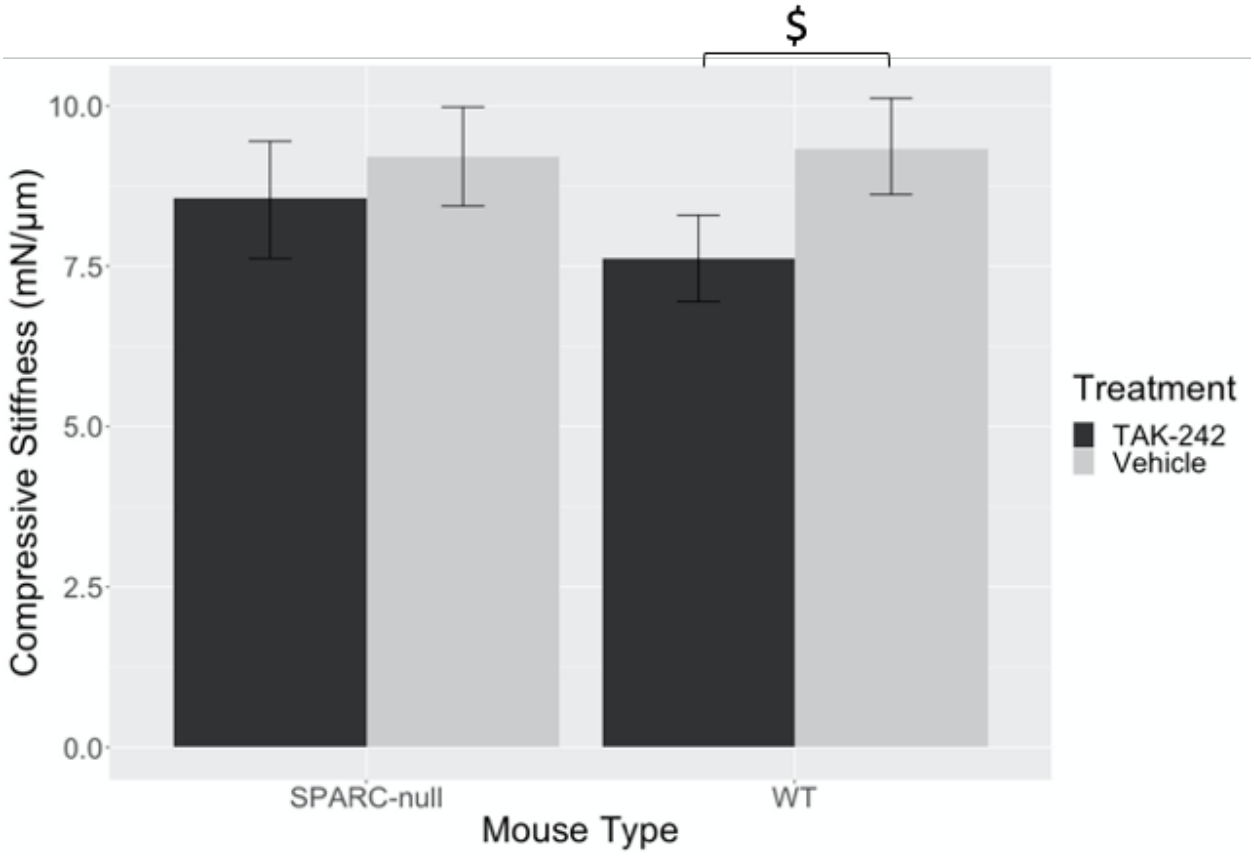

Figure 12: Mean compressive stiffness (mN/μm) of SPARC-null and WT groups collapsed across mechanical tests performed with 1,2, and 3 IVDs tested in series. Error bars depict standard deviation. $ denotes statistical significance in WT mice only. A total of 40 spines were tested with n=10 per group, for a total of 120 included tests.

4.4 NZ Length

NZ length was significantly smaller in SPARC-null mice compared to WT (p=0.008), SPARC-null: 225.83 μm (65.47), WT: 256.1 μm (80.66) . There was no effect of treatment on NZ length collapsed across mouse type (p=0.072). Independent mouse type analysis did not reveal an effect TAK-242 treatment in WT or SPARC-null mice (p=0.169 and p=0.816 respectively).

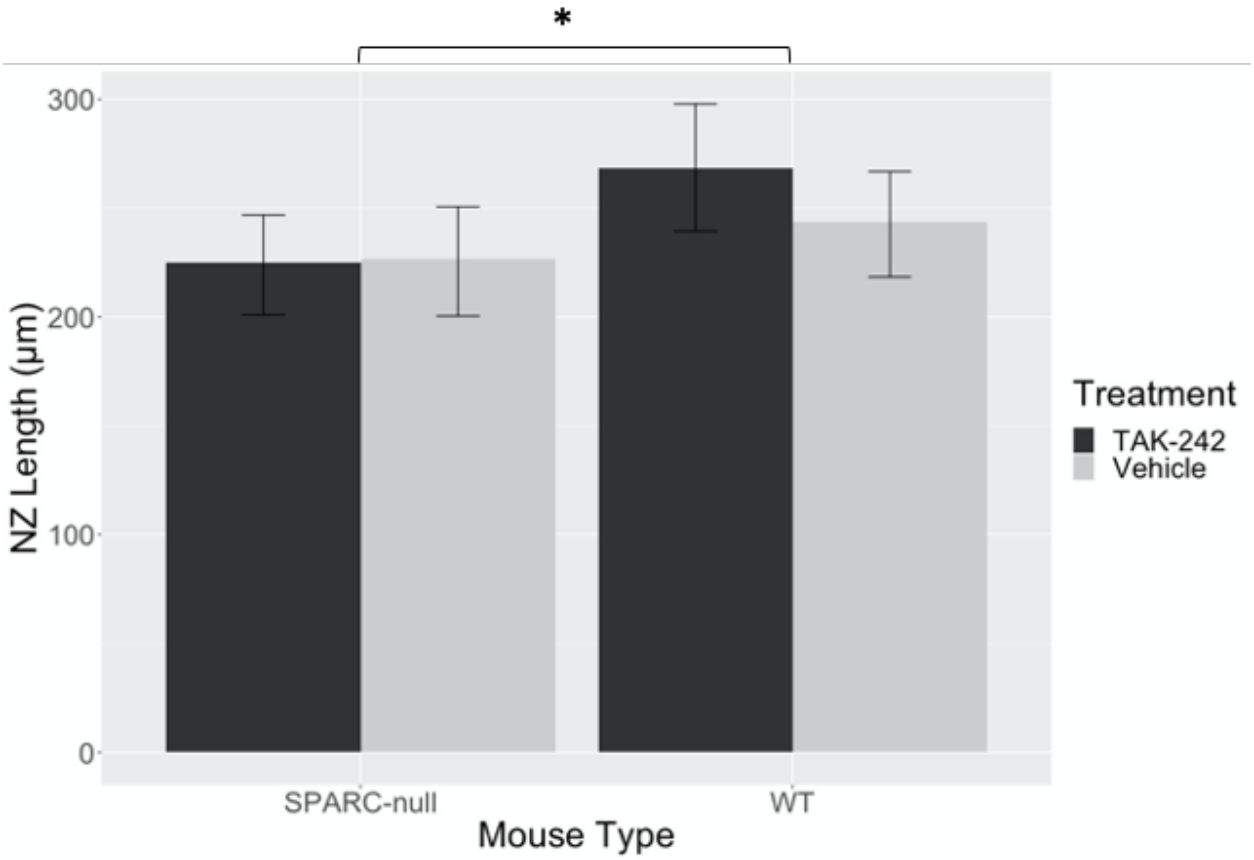

Figure 13: Mean NZ length (μm) of SPARC-null and WT groups collapsed across mechanical tests performed with 1,2, and 3 IVDs tested in series. Error bars depict standard deviation. * denotes statistical significance. A total of 40 spines were tested with n=10 per group, for a total of 120 included tests.

4.5 Hysteresis Energy

Hysteresis energy was significantly greater in mice treated with TAK-242 compared to vehicle ($p=0.036$, TAK-242: 2.94×10^{-4} Nm (8.82×10^{-5}) and vehicle: 2.44×10^{-4} Nm (7.02×10^{-5}). Hysteresis energy was not impacted by mouse type ($p=0.981$). There was no mouse type – treatment interaction, $p=0.634$. Hysteresis energy was directly tied to the number of IVDs tested in series as mean values of 3.14×10^{-4} Nm (8.78×10^{-5}), 2.72×10^{-4} Nm (7.56×10^{-5}), and 2.26×10^{-4} Nm (6.29×10^{-5}) were calculated for levels 3, 2, and 1 respectively.

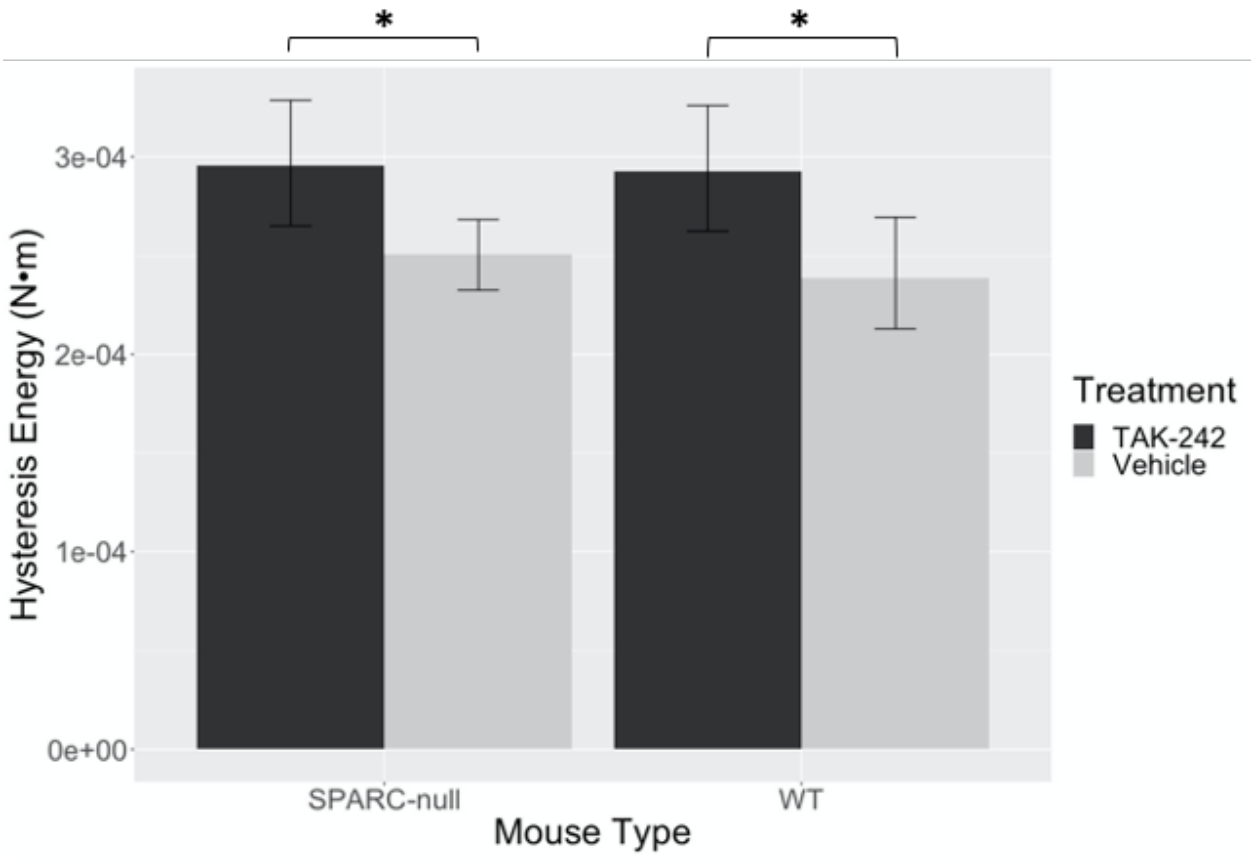

Figure 14: Mean hysteresis energy of SPARC-null and WT groups collapsed across mechanical tests performed with 1,2, and 3 IVDs tested in series. Error bars depict standard deviation. * denotes statistical significance. A total of 40 spines were tested with n=10 per group, for a total of 120 included tests.

4.6 Normalized Hysteresis Energy

Normalized hysteresis was calculated to account for the differences in hysteresis energy due to tissue size and testing ROM. Once normalized, hysteresis energy revealed an effect of mouse type (p=0.025), where hysteresis energy was significantly greater in SPARC-null mice, SPARC-null: 4.54 x 10^{-4} Nm/mm (9.37 x 10^{-5}), WT: 4.15 x 10^{-4} Nm/mm (9.45 x 10^{-5}). Normalized hysteresis energy was also greater in mice treated with TAK-242 (p=0.047, TAK-242: 4.52 x 10^{-4} Nm/mm (9.36 x 10^{-5}) and Vehicle: 4.16 x 10^{-4} Nm/mm (9.56 x 10^{-5})). There was no interaction between mouse type and treatment (p=0.81).

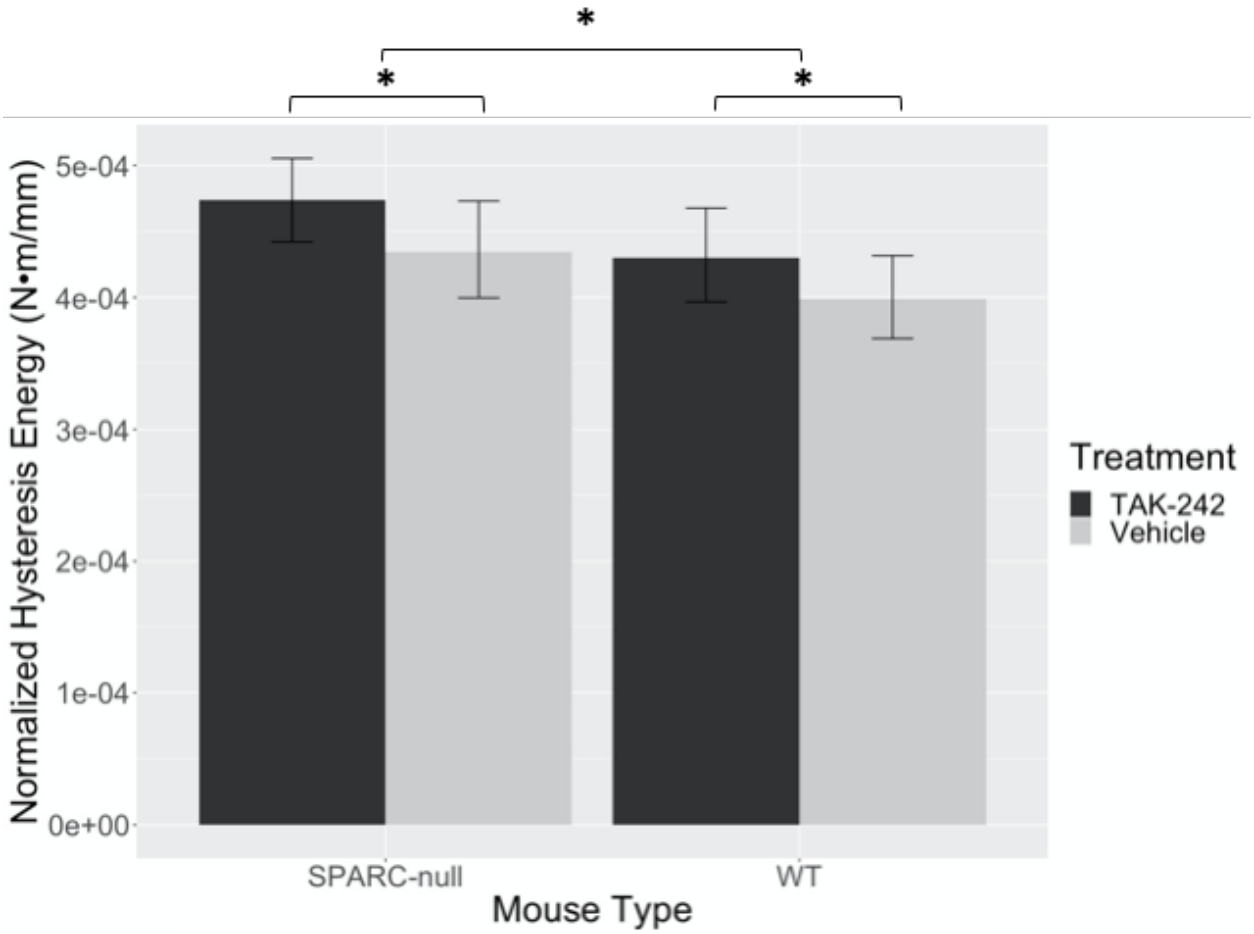

Figure 15: Mean normalized hysteresis energy of SPARC-null and WT groups collapsed across mechanical tests performed with 1,2, and 3 IVDs tested in series. Error bars depict standard deviation. * denotes statistical significance. A total of 40 spines were tested with n=10 per group, for a total of 120 included tests.

5. DISCUSSION

The present study examined the influence of TAK-242 treatment on the mechanical properties of SPARC-null spines. The SPARC-null mouse has been shown to be a good model for intervertebral disc degeneration (Gruber et al., 2005; Krock et al., 2018), and while TAK-242 has been shown to mitigate signs of LBP in SPARC-null mice (Krock et al 2018), the present study did not detect any changes in the NZ mechanical properties of SPARC-null spines as a result of TAK-242 treatment. Therefore, the hypothesis that SPARC-null mice treated with TAK-242 would display similar NZ properties to WT mice injected with saline and WT mice injected with TAK-242 was rejected. Both NZ stiffness and length were not significantly altered by the 8-week administration of TAK-242 in SPARC-null mice. However, as predicted, SPARC-null NZs were significantly stiffer and smaller in length than WT NZs. Tensile stiffness hypotheses were partially correct as stiffness was greater in SPARC-null animals but was not impacted by TAK-242 treatment. Similarly, predictions of compressive stiffness were accurate to find that stiffness was not impacted by TAK-242 treatment with only a near significant effect of mouse type ($p=0.059$). Mice treated with TAK-242 presented with increased hysteresis energy, aligning with hypotheses, in addition to hysteresis energy increasing with the number of IVDs tested in series. Once normalized, hysteresis energy was greater in SPARC-null mice and in mice treated with TAK-242. When separated by mouse type, TAK-242 treatment showed a main effect of reducing NZ and compressive stiffness in WT mice only. TAK-242 treatment did not impact NZ stiffness, NZ length, tensile stiffness and compressive stiffness in SPARC-null mice; indicating a differential effect of TAK-242 based on mouse type (Figure 16).

TLR activation has proven to induce degeneration in human IVDs ex vivo (Krock et al., 2017). Further, chronic TLR4 inhibition via TAK-242 treatment demonstrated decreases in LBP related behaviours, as well as signs of disc degeneration in mice (Krock et al., 2018). Due to the generally accepted hypothesis that altered spinal mechanics leads to LBP (Panjabi, 2003); it was believed that TAK-242 may also be able to revert degenerative changes to IVDs, and restore spinal mechanics. However, chronic TAK-242 administration did not appear to restore spinal NZ mechanics in the current investigation.

IVD NZ properties allow for unconstrained motion with small deformations and stability as stiffness increases at large deformations (Panjabi, 2003). NZ measures have proven sensitive to changes in the state of the IVD and can be used to inform changes in spinal stability (Iatridis et al., 2013; Panjabi, 2003). Changes to NZ length may be more detrimental to loading patterns than changes in NZ stiffness. As the NZ is already the region of minimal stiffness, a change in the minimum stiffness level may not be as impactful to loading as changing the ROM for which minimal stiffness exists. Any change from physiological norm is regarded as potentially harmful (Stokes & Iatridis, 2004) as introducing joint laxity to FSUs allows for aberrant motion to occur; introducing the potential for IVD damage at loads that are normally manageable. Contrastingly, a stiffened motion segment has reduced ROM and altered functional capacity – leading to hypomobility.

Hypothesized Effects of TAK-242 Treatment

WT

Mechanics

TAK-242 treatment introduced compliance to WT IVD NZs

Within WT mice, TAK-242 treatment caused:

21.25% ↓ NZ Stiffness*
18.24% ↓ Compressive Stiffness*
22.63% ↑ Hysteresis*
7.68% ↑ Normalized Hysteresis Energy*

Inflammation

WT Phenotype: Baseline sterile inflammation, ↓ inflammation relative to SPARC-null

TAK-242 Treatment: Decreases baseline TLR4 signalling relative to vehicle

↓ Proinflammatory cytokines
↑ Anti-inflammatory cytokines

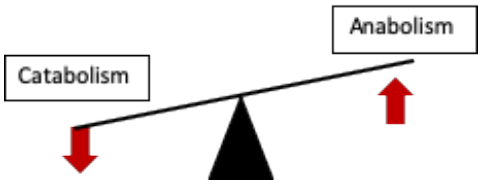

Degeneration

Typical age-dependent degeneration. No herniations, proper fibrous protein regulation, increased disc height, and decreased wedging relative to SPARC-null[1,2]

Hypothesized increase in ECM fibrous protein content due to increased anabolic signalling through reduced inflammation

SPARC-null

Mechanics

TAK-242 treatment did not significantly alter SPARC-null IVD NZ properties. Overall blunted effect of TAK-242 treatment

Within SPARC-null mice, TAK-242 treatment caused:

19.97% ↑ Hysteresis*
9.01% ↑ Normalized Hysteresis Energy*

Inflammation

SPARC-null Phenotype: ↑ Sterile inflammation compared to WT

TAK-242 Treatment: Decreases elevated TLR4 signalling[1] relative to vehicle

↓ Proinflammatory cytokines
↑ Anti-inflammatory cytokines

Degeneration

Accelerated model of IVD degeneration[2] with altered regulation of fibrous proteins critical to ECM composition

SPARC-null IVD displays reduced disc height, wedging, herniations, and proteoglycan loss[2]

No expected attenuation of degenerative changes due to blunted effect of TAK-242 treatment and no changes in disc height index[1]

Figure 16: Summary of the differing mechanical responses of each mouse type to TAK-242 treatment as well as the hypothesized differences in inflammation and degeneration. Listed percent changes are relative to the vehicle treatment (control) within each mouse type. An asterisk denotes results that were found to be statistically significant at the $\alpha = 0.05$ level. [1]Krock et al. 2018, [2] Gruber et al. 2005.

NZ length decreased and NZ stiffness increased as a result of the induced degeneration SPARC-null model despite no effect of TAK-242. Differences in NZ stiffness between segmental levels was not expected as previous research found nearly uniform stiffness across testing levels (Whittal et al., 2020). Previous research identified that decreases in NZ stiffness and reductions in NZ length are typical at the onset of IVD degeneration (Brown, Holmes, & Heiner, 2002; Fujiwara et al., 2000; Hasegewa et al., 2009; Kirkaldy-Willis & Farfan, 1982; Mimura et al., 1994), with additional evidence to suggest that stiffness increases at later stages of degeneration (Brown et al., 2002; Whittal et al., 2020). SPARC-null spines in the current investigation were found to have NZs that were smaller and stiffer than WT counterparts, aligning with previous work (Whittal et al., 2020). Previous characterization of SPARC-null NZs found average stiffness values of 1.91 mN/μm and 1.51 mN/μm for SPARC-null and WT respectively (Whittal et al., 2020). Although both of these values are greater than the 1.81 mN/μm and 1.41 mN/μm of SPARC-null and WT of the current experiment, both comparisons saw nearly identical increases in stiffness in SPARC-null spines relative to WT. Previous data found a 26.5% increase in NZ stiffness in SPARC-null spines compared to the 26.6% increase in the current experiment. Similarly, NZ length was 10.7% smaller (SPARC-null: 259.50 μm, WT: 290.77 μm) in SPARC-null spines in previous research; which also compared well to the 11.8% smaller SPARC-null NZs in the current investigation (SPARC-null: 225.83 μm, WT: 256.1 μm). Despite the similar changes between mouse type NZ properties, it should be noted that the mice utilized by Whittal et al. 2020 were much older with mean ages of 18.86 months (SPARC-null) and 19.52 months (WT) and did not receive any treatment injections. These data suggest that SPARC-null IVDs were likely severely degenerated as NZ laxity is typically the initial result of degeneration.

Supplementary factors that could have also contributed to a stiffened motion segment include ossification, altered hydration, or IVD wedging.

Tensile stiffness was also significantly greater in SPARC-null animals; indicating an effect of degeneration. Although tensile stiffness is not seemingly as important to load bearing as compressive stiffness, the AF must possess sufficient tensile strength to contain the nucleus; allowing for sufficient intradiscal pressure required for load bearing. A comparison of old and young mice (4-5 months vs 20-22) lumbar spines found that degeneration decreased tensile stiffness in the lumbar region but increased in stiffness in the coccygeal region (Holguin et al., 2014). Although contrary to the findings of the current investigation, the mice in Holguin et al. 2014 were degenerated naturally, rather than with an induced degeneration model like the SPARC-null mouse. The degree of degeneration undergone by each group of mice is unclear; which may impact mechanical properties. It is plausible that the degree of degeneration was greater in the SPARC-null mice than the mice examined in the work by Holguin et al., 2014. Axial tensile testing of AF samples has revealed increased stiffness in radial samples (O'Connell et al., 2009) and circumferential-axial samples (Sen et al., 2012) – while quasistatic axial testing found no differences in AF tensile modulus as a result of degeneration (Acaroglu et al., 1995). Sufficient compressive stiffness is vital to force acceptance and transfer through the spinal column. Compressive load bearing depends on proper pressurization of the NP and interlamellar shear resistance of AF layers (Adam et al., 2015; Cannella et al., 2008). Compressive stiffness was not significantly impacted by degeneration, despite reaching near significance at the $\alpha = 0.05$ level ($p=0.059$). Surrounding literature is not clear as to the effect of degeneration on compressive stiffness. A mouse model did not observe any changes in compressive stiffness as a

result of degeneration (Holguin et al., 2014), while human cadaveric analysis measured a decrease in compressive stiffness (Arturo González Gutiérrez, Rangel Alonso, & Gustavo Zambrano Rosas, 2015).

Contrary to NZ mechanics, hysteresis energy was impacted by TAK-242 treatment. Both raw hysteresis energy and normalized hysteresis energy displayed an effect of TAK-242 treatment, with normalized hysteresis additionally affected by mouse type due to degeneration from SPARC gene knockout. In addition to TAK-242 treatment causing increased energy dissipation, hysteresis energy was also greater when more IVDs were tested in series. This was an expected result for normalized hysteresis as the loading of additional IVD tissues provides more opportunities for the interaction of ECM macromolecules, and therefore more opportunities for loss of energy. Hysteresis without normalization was expected to be greater with more IVDs tested in series due to greater testing displacements, and hence, a larger area within a force-displacement curve. Surrounding literature has found that hysteresis energy decreases as a result of degeneration in axial compression (Kazarian, 1975; Nuckley et al., 2008). Further analysis of hysteresis in applied moment mechanical testing has produced mixed results with the exception of degeneration having no impact on hysteresis in flexion-extension testing (Muriuki et al., 2016; Zirbel et al., 2013). In this context, it was surprising to see that normalized hysteresis energy was greater in SPARC-null mice. SPARC-null mice have been validated as a model for IVD degeneration (Gruber et al., 2005; Krock et al., 2018) with additional evidence to suggest that SPARC-null IVDs are highly degeneration (Brown et al., 2002; Whittal et al., 2020). However, characterization of AF fibril morphology in SPARC-null IVDs found a greater range in collagen fibril diameter than WT, accompanied by irregular collagen fibril margins (Gruber et al., 2005).

The orientation of collagen fibrils in SPARC-null IVDs was described as having irregular packing; lacking the fibril uniformity of WT IVDs (Gruber et al., 2005). The irregular and overlapping structure of SPARC-null collagen may be responsible for increased hysteresis among SPARC-null tests as the deformation of such collagen networks would likely induce increased friction and energy loss compared to uniformly aligned AF collagen in WT IVDs.

5.1 SPARC Gene Knockout, TAK-242, and NZ Mechanics

NZ stiffness, compressive stiffness, tensile stiffness, and NZ length were not impacted by TAK-242 treatments in SPARC-null mice (Figure 16). Similar to previous investigations, SPARC-null mice displayed stiffer and smaller NZs compared to WT mice (Whittal et al., 2020). IVD degeneration is a complex catabolic process regulated by a multitude of factors; including genetic manipulations in the current experiment. Hence, the importance of the interaction between SPARC gene knockout, TAK-242 administration and inflammation.

IVD degeneration is a cell-mediated response that is often characterized by the breakdown and fragmentation of the ECM. Fragmented debris of the ECM, termed DAMPs or alarmins, bind at surface TLRs and initiate signalling cascades in the inflammatory response (Krock et al., 2018). Inflammatory cytokines, proteases, and neurotrophins are released as a result of the inflammatory response and contribute to the innervation, sensitization, and overall catabolic state of the ECM (Alkhatib et al., 2014; Basbaum et al., 2009). Acute inflammation assists in the healing process, however, chronic and uncontrolled inflammation results in a feedforward response whereby the release of proinflammatory compounds further contributes to IVD degeneration and causes continued activation of the inflammatory response. TAK-242

selectively binds to TLR4, a transmembrane protein common to many DAMPs (Kuzmich et al., 2017). TAK-242 binds to the intracellular domain of TLR4 at the Cys747 site – preventing the normal cascade of events leading to the release of inflammatory compounds in response to a DAMP (Matsunaga et al., 2011). In effect, TAK-242 prevents a portion of the full inflammatory response in hopes of breaking the positive feedback loop of inflammation and IVD degeneration.

SPARC is a matricellular protein that has a regulatory role in the formation and homeostasis of the ECM (Bradshaw, 2009). Internalized SPARC is released to the outside of cells where high Ca^{2+} concentrations activate its chaperone activity (Bradshaw, 2009; Chlenski et al., 2011). While active, SPARC interacts with surface matrix proteins – namely collagen – to modulate ECM production (Brekken & Sage, 2000; Emerson, Sage, Ghosh, & Clark, 2006). Functional analysis of SPARC revealed that it prevents the formation of collagen fibrils, directs the internalization of its protein targets, and mediates degradation of pre-existing ECM networks (Amy D. Bradshaw, 2009).

It may seem unusual that SPARC-null organisms display increased IVD degeneration as SPARC itself is partly responsible for the degradation of ECM collagen networks. However, the scavenger activity of SPARC might provide the necessary function to maintain the proper composition of the ECM and repair matrix abnormalities during remodelling and growth (Chlenski et al., 2011). SPARC-null mouse IVDs present with altered numbers of disc cells, altered collagen fibril diameters, reduced type I annular collagen, disc wedging, and increased occurrence of herniations in older mice (Gruber et al., 2005). In response to TAK-242 treatment, SPARC-null mice did not recover disc height (Krock et al., 2018), indicating that TAK-242 was

not able to revert degenerative changes (Figure 16). Due to the importance of SPARC in ECM homeostasis, a SPARC-null animal may not be able to regulate ECM production and remodelling as effectively. As a result, the reduced inflammatory response from TAK-242 treatment may not allow for the full attenuation of degenerative changes in SPARC-null organisms. RNA sequencing analysis could provide additional insight as to what genes were differentially expressed in WT and SPARC-null animals that received TAK-242 – aiding in the explanation of the blunted effects of TAK-242 in SPARC-null organisms.

Interestingly, no mechanical variables measured were impacted by TAK-242 treatment in SPARC-null mice. NZ and compressive stiffness of WT mice were significantly reduced through TAK-242 TLR4 inhibition. As WT mice do not experience the heightened inflammatory response and hampered ECM regulation of SPARC-null mice, it is possible that a reduced state of inflammation could impact axial mechanical properties. Inhibiting physiologically normal inflammation in WT mice could have reduced signalling for the initiation of ECM tissue remodelling, leading to a destabilizing effect, or reduction in NZ stiffness, similar to the onset of IVD degeneration. Rationale for this proposed mechanism stems from inflammation playing a key role in the signalling for tissue homeostasis; whereby changes above or below the physiological norm could manifest altered mechanical properties. It is evident that TAK-242 treatment dissimilarly affected mechanics between mouse types. The comparison of TAK-242 and vehicle treatments in WT animals displayed mechanical differences that aligned with initial hypotheses of TAK-242 treatment in SPARC-null animals. It was expected that TAK-242 animals would display decreased NZ stiffness and increased NZ length compared to SPARC-null animals receiving the vehicle treatment, as well as both treatment groups of WT animals. This

assumption was perhaps naïve as current data shows that not only were the effects of TAK-242 somehow blunted in SPARC-null animals, but that TAK-242 also produced measurable differences in WT animals.

5.2 TLR4 signalling, ECM, and hysteresis

Despite not impacting NZ measures in SPARC-null mice, chronic treatment with TAK-242 increased hysteresis energy, independent of mouse type. Hysteresis energy during cyclic biomechanical loading gives a representation of the amount of energy dissipated by the IVD (Lundon et al., 2001; Nuckley et al., 2008). The effect of TAK-242 on hysteresis energy aligned with initial hypotheses but was a surprising result after no differences in NZ properties were found as a result of treatment. The question then becomes; why was hysteresis impacted by TAK-242 treatment? To explore potential explanations, a greater examination of TLR4 signalling and ECM catabolism would be required.

Indeed, the complex biological interactions of catabolic ECM enzymes, their inhibitors, inflammation, and SPARC gene knockout would greatly benefit from RNA sequencing analysis. For example, gene expression analysis of various anabolic and catabolic ECM markers among other newly investigated IVD degeneration markers (Lv et al., 2016) would help contextualize mechanical results and provide greater insight to the effects of TAK-242 on IVDs. With the current available information, it is possible to hypothesize that the inhibition of TLR4 signalling could have led to an accumulation of additional ECM material in mice treated with TAK-242 and differences in hysteresis energy. Material inefficiencies and energy loss due to friction is

common in viscoelastic biological tissues. It is possible that greater accumulations of ECM material due to TAK-242 treatment – such as the highly fibrous protein collagen – caused greater energy dissipation when loaded as a result of increased friction from fibrous ECM matter. Despite the interesting findings of hysteresis energy, TAK-242 did not influence NZ mechanics. It may also be possible that hysteresis energy is a more sensitive measure than NZ stiffness and length.

5.3 Limitations and Future Directions

This work must be taken with a number of considerations. The assumption of degeneration being present in SPARC-null spines relies on previous data and the mechanical testing results of the current analysis for which the degree of IVD degeneration is unclear. Additionally, the presence of minor herniations could have altered the mechanics of SPARC-null IVDs as previous research identified major herniations in 14,19, and 20 month old SPARC-null mice (Gruber et al., 2005). It is however unlikely that major herniations were present within the tested lumbar spines as tensile mechanical testing of a severely herniated disc may not allow for the production of a tensile toe-region in force-displacement data. In the event that TAK-242 does have potential to attenuate degenerative changes to IVDs, it is possible that the provided treatment was too short, not implemented at the proper stage of degeneration, or not administered at the necessary dosage. Krock et al. 2018 found that TAK-242 only improved behavioural signs of LBP during weeks 4-8 of treatment, so it may be possible to elucidate greater mechanical changes with a longer duration of treatment.

As SPARC-null mice experience LBP at around 2 months of age (Millecamps et al., 2012), and were tested at a minimum age of 7.5 months, the chance of recovering degenerative changes to IVDs was small. Future research should examine earlier intervention with TAK-242 to examine the possibility of preventing degenerative changes associated with IVD degeneration at its onset. Additionally, future measurement of axial IVD mechanics may benefit from testing more than a single IVD in series. Variability in NZ stiffness was greatest when only a single IVD was tested, in addition to previous work showing that the ability to detect differences between experimental conditions increased as the number of IVDs tested in series increased (Whittal et al., 2020). Effects of TAK-242 should also be tested on other models of IVD degeneration, perhaps an aged WT mouse model as the SPARC-null model in the current investigation showed a blunted effect of TAK-242 on SPARC-null NZ mechanics. Future gene expression analysis of the experimental population would provide great insight to the differing mechanical responses of WT and SPARC-null to TAK-242 treatment. Targets of interest for expression analysis include TLR signalling and ECM associated genes and proteins like MMPs, ADAMTSs, uPA,uPAR, COL-2, and AGC among other IVD degeneration markers (Lv et al., 2016). Pain signalling can also be inferred from expression levels of microglia and astrocytes.

5.4 Conclusion

In conclusion, while SPARC-null spines were found to have smaller and stiffer NZs than WT spines, TAK-242 treatment was not able to impact these measures in SPARC-null mice. Interestingly, TAK-242 did impact hysteresis energy, indicating that hysteresis might be a more sensitive measure to detect changes to the IVD state. Tensile stiffness was greater in SPARC-null animals but both tensile and compressive stiffness were not impacted by TAK-242 in

SPARC-null mice. TAK-242 treatment reduced NZ and compressive stiffness in WT, but not SPARC-null mice; advocating that there may have been a blunted effect of TAK-242 treatment in SPARC-null mice. TLR inhibitors, such as TAK-242, possess potential as a therapeutic for LBP and should be further investigated in a variety of degenerated animal models for their ability to slow or modify chronic pain and IVD function.

References

Acaroglu, E. R., Latridis, J. C., Setton, L. A., Foster, R. J., Mow, V. C., & Weidenbaum, and M. (1995). Degeneration and Aging Affect the Tensile Behavior of Human Lumbar Anulus Fibrosus. *Spine*, *20*(24), 2690–2701. https://doi.org/10.1097/00007632-199512150-00010

Adam, C., Rouch, P., & Skalli, W. (2015). Inter-lamellar shear resistance confers compressive stiffness in the intervertebral disc: An image-based modelling study on the bovine caudal disc. *Journal of Biomechanics*, *48*(16), 4303–4308. https://doi.org/10.1016/j.jbiomech.2015.10.041

Adams, M A, Mcnally, S., Dolan, P., & Mcnally, D. S. (1996). *"STRESS" DISTRIBUTIONS INSIDE INTERVERTEBRAL DISCS THE EFFECTS OF AGE AND DEGENERATION*. *J Bone Joint Surg [Br]* (Vol. 78). Retrieved from https://online.boneandjoint.org.uk/doi/pdf/10.1302/0301-620X.78B6.0780965

Adams, Michael A., & Roughley, P. J. (2006). What is Intervertebral Disc Degeneration, and What Causes It? *Spine*, *31*(18), 2151–2161. https://doi.org/10.1097/01.brs.0000231761.73859.2c

Adams, Michael A., Stefanakis, M., & Dolan, P. (2010). Healing of a painful intervertebral disc should not be confused with reversing disc degeneration: Implications for physical therapies for discogenic back pain. *Clinical Biomechanics*, *25*(10), 961–971. https://doi.org/10.1016/j.clinbiomech.2010.07.016

Alkhatib, B., Rosenzweig, D. H., Krock, E., Roughley, P. J., Beckman, L., Steffen, T., … Haglund, L. (2014). Acute mechanical injury of the human intervertebral disc: link to degeneration and pain. *European Cells & Materials*, *28*, 98–110; discussion 110-1. Retrieved from http://www.ncbi.nlm.nih.gov/pubmed/25214017

Amelot, A., & Mazel, C. (2018). The intervertebral disc: physiology and pathology of a brittle joint. *World Neurosurgery*. https://doi.org/10.1016/j.wneu.2018.09.032

Arturo González Gutiérrez, R., Rangel Alonso, V., & Gustavo Zambrano Rosas, J. (2015). Biomechanics of the Intervertebral Disc in Compression: Experimental and Numerical Study. *Journal of Mechanics Engineering and Automation*, *5*, 39–44. https://doi.org/10.17265/2159-5275/2015.01.006

Balkovec, C., Adams, M. A., Dolan, P., & Mcgill, S. M. (2015). Annulus Fibrosus Can Strip Hyaline Cartilage End Plate from Subchondral Bone: A Study of the Intervertebral Disk in Tension. *Global Spine J*, *5*, 360–365. https://doi.org/10.1055/s-0035-1546956

Barker, T. H., Baneyx, G., Cardó-Vila, M., Workman, G. A., Weaver, M., Menon, P. M., … Sage, E. H. (2005). SPARC regulates extracellular matrix organization through its modulation of integrin-linked kinase activity. *Journal of Biological Chemistry*, *280*(43), 36483–36493. https://doi.org/10.1074/jbc.M504663200

Basbaum, A. I., Bautista, D. M., Scherrer, G., & Julius, D. (2009). Cellular and Molecular Mechanisms of Pain. *Cell*, *139*(2), 267–284. https://doi.org/10.1016/J.CELL.2009.09.028

Beckstein, J. C., Sen, S., Schaer, T. P., Vresilovic, E. J., & Elliott, D. M. (2008). Comparison of Animal Discs Used in Disc Research to Human Lumbar Disc. *Spine*, *33*(6), E166–E173. https://doi.org/10.1097/BRS.0b013e318166e001

Bornstein, P. (2009). Matricellular proteins: an overview. *Journal of Cell Communication and Signaling*, *3*(3–4), 163–165. https://doi.org/10.1007/s12079-009-0069-z

Bornstein, P., & Sage, E. H. (2002). Matricellular proteins: extracellular modulators of cell

function. *Current Opinion in Cell Biology*, *14*(5), 608–616. https://doi.org/10.1016/S0955-0674(02)00361-7

Bradshaw, A D, & Sage, E. H. (2001). SPARC, a matricellular protein that functions in cellular differentiation and tissue response to injury. *The Journal of Clinical Investigation*, *107*(9), 1049–1054. https://doi.org/10.1172/JCI12939

Bradshaw, Amy D. (2009, October 2). The role of SPARC in extracellular matrix assembly. *Journal of Cell Communication and Signaling*. Springer. https://doi.org/10.1007/s12079-009-0062-6

Brekken, R. A., & Sage, E. H. (2000). SPARC, a matricellular protein: at the crossroads of cell-matrix. *Matrix Biology : Journal of the International Society for Matrix Biology*, *19*(7), 569–580. https://doi.org/10.1016/s0945-053x(00)00105-0

Brinckmann, P., & Grootenboer, H. (1991). Change of disc height, radial disc bulge, and intradiscal pressure from discectomy. An in vitro investigation on human lumbar discs. *Spine*, *16*(6), 641–646. Retrieved from http://www.ncbi.nlm.nih.gov/pubmed/1862403

Brown, M. D., Holmes, D. C., & Heiner, A. D. (2002). Measurement of cadaver lumbar spine motion segment stiffness. *Spine*, *27*(9), 918–922. Retrieved from http://www.ncbi.nlm.nih.gov/pubmed/11979161

Brown, S. H. M., Gregory, D. E., & McGill, S. M. (2008). Vertebral end-plate fractures as a result of high rate pressure loading in the nucleus of the young adult porcine spine. *Journal of Biomechanics*, *41*(1), 122–127. https://doi.org/10.1016/j.jbiomech.2007.07.005

Buckwalter, J. A. (1995). Aging and degeneration of the human intervertebral disc. *Spine*, *20*(11), 1307–1314. Retrieved from http://www.ncbi.nlm.nih.gov/pubmed/7660243

Bussières, A. E., Stewart, G., Al-Zoubi, F., Decina, P., Descarreaux, M., Haskett, D., … Ornelas, J. (2018). Spinal Manipulative Therapy and Other Conservative Treatments for Low Back Pain: A Guideline From the Canadian Chiropractic Guideline Initiative. *Journal of Manipulative and Physiological Therapeutics*, *41*(4), 265–293. https://doi.org/10.1016/j.jmpt.2017.12.004

Cannella, M., Arthur, A., Allen, S., Keane, M., Joshi, A., Vresilovic, E., & Marcolongo, M. (2008). The role of the nucleus pulposus in neutral zone human lumbar intervertebral disc mechanics. *Journal of Biomechanics*, *41*(10), 2104–2111. https://doi.org/10.1016/j.jbiomech.2008.04.037

Chlenski, A., Guerrero, L. J., Salwen, H. R., Yang, Q., Tian, Y., la Madrid, A., … Cohn, S. L. (2011). Secreted protein acidic and rich in cysteine is a matrix scavenger chaperone. *PLoS ONE*, *6*(9), e23880. https://doi.org/10.1371/journal.pone.0023880

Choi, K. S., Cohn, M. J., & Harfe, B. D. (2008). Identification of nucleus pulposus precursor cells and notochordal remnants in the mouse: Implications for disk degeneration and chordoma formation. *Developmental Dynamics*, *237*(12), 3953–3958. https://doi.org/10.1002/dvdy.21805

Chow, D. H. K., Luk, K. D. K., Holmes, A. D., Li, X. F., & Tam, S. C. W. (2004). Multi-planar bending properties of lumbar intervertebral joints following cyclic bending. *Clinical Biomechanics*, *19*(2), 99–106. https://doi.org/10.1016/j.clinbiomech.2003.11.001

De Souza, A. P., Vale, V. L. C., Silva, M. D. C., Araújo, I. B. D. O., Trindade, S. C., Moura-Costa, L. F. De, … Meyer, R. (2014). MAPK involvement in cytokine production in response to Corynebacterium pseudotuberculosis infection. *BMC Microbiology*, *14*(1), 230. https://doi.org/10.1186/s12866-014-0230-6

Ebara, S., Iatridis, J. C., Setton, L. A., Foster, R. J., Mow, V. C., & Weidenbaum, M. (1996).

Tensile properties of nondegenerate human lumbar anulus fibrosus. *Spine*, *21*(4), 452–461. Retrieved from http://www.ncbi.nlm.nih.gov/pubmed/8658249

Edgar, M. A. (2007). The nerve supply of the lumbar intervertebral disc. *The Journal of Bone and Joint Surgery. British Volume*, *89-B*(9), 1135–1139. https://doi.org/10.1302/0301-620X.89B9.18939

Elliott, D. M., & Sarver, J. J. (2004). Young investigator award winner: validation of the mouse and rat disc as mechanical models of the human lumbar disc. *Spine*, *29*(7), 713–722. Retrieved from http://www.ncbi.nlm.nih.gov/pubmed/15087791

Emerson, R. O., Sage, E. H., Ghosh, J. G., & Clark, J. I. (2006). Chaperone-like activity revealed in the matricellular protein SPARC. *Journal of Cellular Biochemistry*, *98*(4), 701–705. https://doi.org/10.1002/jcb.20867

Erwin, W., Islam, D., Inman, R. D., Fehlings, M. G., & Tsui, F. W. (2011). Notochordal cells protect nucleus pulposus cells from degradation and apoptosis: implications for the mechanisms of intervertebral disc degeneration. *Arthritis Research & Therapy*, *13*(6), R215. https://doi.org/10.1186/ar3548

Fan, S. C., Ghista, D. N., Sridhar, I., & Ramakrishna, K. (2005). Biomechanics of the Intrinsically Optimal Design of the Intervertebral Disc. In *2005 IEEE Engineering in Medicine and Biology 27th Annual Conference* (Vol. 4, pp. 4408–4411). IEEE. https://doi.org/10.1109/IEMBS.2005.1615443

Fox, J., Davisson, M., Quimby, F., Barthold, S., Newcomer, C., & Smith, A. (Eds.). (2007). *The Mouse in Biomedical Research : Immunology* (2nd ed., Vol. 4). Elsevier. Retrieved from http://web.b.ebscohost.com.libproxy.wlu.ca/ehost/ebookviewer/ebook/ZTAwMHhuYV9fMTg2MDU5X19BTg2?sid=d574b8bb-9f7e-4df8-8f9c-3f2a250918d8@pdc-v-sessmgr02&vid=0&format=EB&lpid=lp_303&rid=0

Fraser, R. D., Osti, O. L., & Vernon-Roberts, B. (1993). Intervertebral disc degeneration. *European Spine Journal : Official Publication of the European Spine Society, the European Spinal Deformity Society, and the European Section of the Cervical Spine Research Society*, *1*(4), 205–213. https://doi.org/10.1007/bf00298361

Freemont, A., Peacock, T., Goupille, P., Hoyland, J., O'Brien, J., & Jayson, M. (1997). Nerve ingrowth into diseased intervertebral disc in chronic back pain. *The Lancet*, *350*(9072), 178–181. https://doi.org/10.1016/S0140-6736(97)02135-1

Fujiwara, A., Lim, T. H., An, H. S., Tanaka, N., Jeon, C. H., Andersson, G. B., & Haughton, V. M. (2000). The effect of disc degeneration and facet joint osteoarthritis on the segmental flexibility of the lumbar spine. *Spine*, *25*(23), 3036–3044. Retrieved from http://www.ncbi.nlm.nih.gov/pubmed/11145815

García-Cosamaló, J., Del Valle, M. E., Calavia, M. G., García-Suá Rez, O., Ló Pez-Muñ, A., Otero, J. S., & Vega, J. A. (2010). Intervertebral disc, sensory nerves and neurotrophins: who is who in discogenic pain? *Journal of Anatomy*, 1–15. https://doi.org/10.1111/j.1469-7580.2010.01227.x

Gardner-Morse, M. G., & Stokes, I. A. (2003). Physiological axial compressive preloads increase motion segment stiffness, linearity and hysteresis in all six degrees of freedom for small displacements about the neutral posture. *Journal of Orthopaedic Research*, *21*(3), 547–552. https://doi.org/10.1016/S0736-0266(02)00199-7

Gregory, D. E., Bae, W. C., Sah, R. L., & Masuda, K. (2012). Anular delamination strength of human lumbar intervertebral disc. *European Spine Journal*, *21*(9), 1716–1723. https://doi.org/10.1007/s00586-012-2308-x

Gruber, H. E., Ingram, J. A., Leslie, K., & Hanley, E. N. (2004). Cellular, but not matrix, immunolocalization of SPARC in the human intervertebral disc: decreasing localization with aging and disc degeneration. *Spine*, *29*(20), 2223–2228. Retrieved from http://www.ncbi.nlm.nih.gov/pubmed/15480132

Gruber, H. E., Sage, E. H., Norton, H. J., Funk, S., Ingram, J., & Hanley, E. N. (2005). Targeted Deletion of the SPARC Gene Accelerates Disc Degeneration in the Aging Mouse. *Journal of Histochemistry & Cytochemistry*, *53*(9), 1131–1138. https://doi.org/10.1369/jhc.5A6687.2005

Gsell, K. Y., Zwambag, D. P., Fournier, D. E., Séguin, C. A., & Brown, S. H. M. (2017). Paraspinal Muscle Passive Stiffness Remodels in Direct Response to Spine Stiffness. *SPINE*, *42*(19), 1440–1446. https://doi.org/10.1097/BRS.0000000000002132

Hasegewa, K., Kitahara, K., Hara, T., Takano, K., & Shimoda, H. (2009). Biomechanical evaluation of segmental instability in degenerative lumbar spondylolisthesis. *European Spine Journal*, *18*(4), 465–470. https://doi.org/10.1007/s00586-008-0842-3

Hauerstock, *, Reindl, R. ; +, & Steffen. (2001). *TELEMETRIC MEAUREMENT OF COMPRESSIVE LOADS IN THE SHEEP LUMBAR SPINE*. *Orthopaedic Research Society*. Retrieved from http://www.ors.org/Transactions/47/0931.pdf

Hayes, A. J., Benjamin, M., & Ralphs, J. R. (2001). Extracellular matrix in development of the intervertebral disc. *Matrix Biology : Journal of the International Society for Matrix Biology*, *20*(2), 107–121. Retrieved from http://www.ncbi.nlm.nih.gov/pubmed/11334712

Holguin, N., Aguilar, R., Harland, R. A., Bomar, B. A., & Silva, M. J. (2014). The aging mouse partially models the aging human spine: Lumbar and coccygeal disc height, composition, mechanical properties, and Wnt signaling in young and old mice. *Journal of Applied Physiology*, *116*(12), 1551–1560. https://doi.org/10.1152/japplphysiol.01322.2013

Hoy, D., Bain, C., Williams, G., March, L., Brooks, P., Blyth, F., … Buchbinder, R. (2012). A systematic review of the global prevalence of low back pain. *Arthritis & Rheumatism*, *64*(6), 2028–2037. https://doi.org/10.1002/art.34347

Hoy, D., March, L., Brooks, P., Blyth, F., Woolf, A., Bain, C., … Buchbinder, R. (2014). The global burden of low back pain: estimates from the Global Burden of Disease 2010 study. *Annals of the Rheumatic Diseases*, *73*(6), 968–974. https://doi.org/10.1136/annrheumdis-2013-204428

Hutton, W. C., Ganey, T. M., Elmer, W. A., Kozlowska, E., Ugbo, J. L., Doh, E. S., & Whitesides, T. E. (2000). Does long-term compressive loading on the intervertebral disc cause degeneration? *Spine*, *25*(23), 2993–3004. Retrieved from http://www.ncbi.nlm.nih.gov/pubmed/11145810

Iatridis, J. C., Nicoll, S. B., Michalek, A. J., Walter, B. A., & Gupta, M. S. (2013). Role of biomechanics in intervertebral disc degeneration and regenerative therapies: what needs repairing in the disc and what are promising biomaterials for its repair? *The Spine Journal*, *13*(3), 243–262. https://doi.org/10.1016/J.SPINEE.2012.12.002

Ii, M., Matsunaga, N., Hazeki, K., Nakamura, K., Takashima, K., Seya, T., … Iizawa, Y. (2006). A Novel Cyclohexene Derivative, Ethyl (6R)-6-[N-(2-Chloro-4-fluorophenyl)sulfamoyl]cyclohex-1-ene-1-carboxylate (TAK-242), Selectively Inhibits Toll-Like Receptor 4-Mediated Cytokine Production through Suppression of Intracellular Signaling. *Molecular Pharmacology*, *69*(4), 1288–1295. https://doi.org/10.1124/MOL.105.019695

Inoue, H. (1981). Three-dimensional architecture of lumbar intervertebral discs. *Spine*, *6*(2),

139–146. Retrieved from http://www.ncbi.nlm.nih.gov/pubmed/7280814
Inoue, N., & Espinoza Orías, A. A. (2011). Biomechanics of Intervertebral Disk Degeneration. *Orthopedic Clinics of North America*, *42*(4), 487–499. https://doi.org/10.1016/J.OCL.2011.07.001
Jaumard, N. V., Welch, W. C., & Winkelstein, B. A. (2011). Spinal Facet Joint Biomechanics and Mechanotransduction in Normal, Injury and Degenerative Conditions. *Journal of Biomechanical Engineering*, *133*(7), 71010. https://doi.org/10.1115/1.4004493
Johannessen, W., Cloyd, J. M., O'Connell, G. D., Vresilovic, E. J., & Elliott, D. M. (2006). Trans-Endplate Nucleotomy Increases Deformation and Creep Response in Axial Loading. *Annals of Biomedical Engineering*, *34*(4), 687–696. https://doi.org/10.1007/s10439-005-9070-8
Kazarian, L. E. (1975). Creep characteristics of the human spinal column. *The Orthopedic Clinics of North America*, *6*(1), 3–18. Retrieved from http://www.ncbi.nlm.nih.gov/pubmed/1113976
Khan, A. N., Jacobsen, H. E., Khan, J., Filippi, C. G., Levine, M., Lehman, R. A., … Chahine, N. O. (2017). Inflammatory biomarkers of low back pain and disc degeneration: a review. *Annals of the New York Academy of Sciences*, *1410*(1), 68–84. https://doi.org/10.1111/nyas.13551
Kirkaldy-Willis, W. H., & Farfan, H. F. (1982). Instability of the lumbar spine. *Clinical Orthopaedics and Related Research*, (165), 110–123. Retrieved from http://www.ncbi.nlm.nih.gov/pubmed/6210480
Klawitter, M., Hakozaki, M., Kobayashi, H., Krupkova, O., Quero, L., Ospelt, C., … Wuertz, K. (2014). Expression and regulation of toll-like receptors (TLRs) in human intervertebral disc cells. *European Spine Journal*, *23*(9), 1878–1891. https://doi.org/10.1007/s00586-014-3442-4
Krock, E., Currie, J. B., Weber, M. H., Ouellet, J. A., Stone, L. S., Rosenzweig, D. H., & Haglund, L. (2016). Nerve Growth Factor Is Regulated by Toll-Like Receptor 2 in Human Intervertebral Discs. *Journal of Biological Chemistry*, *291*(7), 3541–3551. https://doi.org/10.1074/JBC.M115.675900
Krock, E., Millecamps, M., Currie, J. B., Stone, L. S., & Haglund, L. (2018). Low back pain and disc degeneration are decreased following chronic toll-like receptor 4 inhibition in a mouse model. *Osteoarthritis and Cartilage*, *26*(9), 1236–1246. https://doi.org/10.1016/J.JOCA.2018.06.002
Krock, E., Rosenzweig, D. H., Currie, J. B., Bisson, D. G., Ouellet, J. A., & Haglund, L. (2017). Toll-like receptor activation induces degeneration of human intervertebral discs. *Scientific Reports*, *7*(1), 1–12. https://doi.org/10.1038/s41598-017-17472-1
Kuzmich, N., Sivak, K., Chubarev, V., Porozov, Y., Savateeva-Lyubimova, T., & Peri, F. (2017). TLR4 Signaling Pathway Modulators as Potential Therapeutics in Inflammation and Sepsis. *Vaccines*, *5*(4), 34. https://doi.org/10.3390/vaccines5040034
Lawrence, T. (2009). The nuclear factor NF-kappaB pathway in inflammation. *Cold Spring Harbor Perspectives in Biology*, *1*(6), a001651. https://doi.org/10.1101/cshperspect.a001651
Li, Y., Zhang, H., Kosturakis, A. K., Cassidy, R. M., Zhang, H., Kennamer-Chapman, R. M., … Dougherty, P. M. (2015). MAPK signaling downstream to TLR4 contributes to paclitaxel-induced peripheral neuropathy. *Brain, Behavior, and Immunity*, *49*, 255–266. https://doi.org/10.1016/j.bbi.2015.06.003

Liu, T., Zhang, L., Joo, D., & Sun, S. C. (2017, July 14). NF-κB signaling in inflammation. *Signal Transduction and Targeted Therapy*. Springer Nature. https://doi.org/10.1038/sigtrans.2017.23

Lotz, J. C., Fields, A. J., & Liebenberg, E. C. (2013). The Role of the Vertebral End Plate in Low Back Pain. *Global Spine Journal*, *3*(3), 153–163. https://doi.org/10.1055/s-0033-1347298

Lundon, K., Bolton, K., Diploma, G., & Physiotherapyz, M. (2001). *Structure and Function of the Lumbar Intervertebral Disk in Health, Aging, and Pathologic Conditions*. *Journal of Orthopaedic & Sports Physical Therapy* (Vol. 31). Retrieved from www.jospt.org

Lv, F.-J., Peng, Y., Lim, F. L., Sun, Y., Lv, M., Zhou, L., … Leung, V. Y. L. (2016). Matrix metalloproteinase 12 is an indicator of intervertebral disc degeneration co-expressed with fibrotic markers. *Osteoarthritis and Cartilage*, *24*(10), 1826–1836. https://doi.org/10.1016/j.joca.2016.05.012

Marchand, F., & Ahmed, A. M. (1990). Investigation of the laminate structure of lumbar disc anulus fibrosus. *Spine*, *15*(5), 402–410. Retrieved from http://www.ncbi.nlm.nih.gov/pubmed/2363068

Matsunaga, N., Tsuchimori, N., Matsumoto, T., & Ii, M. (2011). TAK-242 (Resatorvid), a Small-Molecule Inhibitor of Toll-Like Receptor (TLR) 4 Signaling, Binds Selectively to TLR4 and Interferes with Interactions between TLR4 and Its Adaptor Molecules. *Molecular Pharmacology*, *79*(1), 34–41. https://doi.org/10.1124/mol.110.068064

McCann, M. R., Tamplin, O. J., Rossant, J., & Seǵuin, C. A. (2012). Tracing notochord-derived cells using a Noto-cre mouse: Implications for intervertebral disc development. *DMM Disease Models and Mechanisms*, *5*(1), 73–82. https://doi.org/10.1242/dmm.008128

McNally, D. S., & Adams, M. A. (1992). Internal intervertebral disc mechanics as revealed by stress profilometry. *Spine*, *17*(1), 66–73. Retrieved from http://www.ncbi.nlm.nih.gov/pubmed/1536017

Metsäranta, M., Young, M. F., Sandberg, M., Termine, J., & Vuorio, E. (1989). Localization of osteonectin expression in human fetal skeletal tissues by in situ hybridization. *Calcified Tissue International*, *45*(3), 146–152. Retrieved from http://www.ncbi.nlm.nih.gov/pubmed/2505905

Millecamps, M., Czerminski, J. T., Mathieu, A. P., & Stone, L. S. (2015). Behavioral signs of axial low back pain and motor impairment correlate with the severity of intervertebral disc degeneration in a mouse model. *The Spine Journal*, *15*(12), 2524–2537. https://doi.org/10.1016/J.SPINEE.2015.08.055

Millecamps, M., Tajerian, M., Naso, L., Sage, H. E., & Stone, L. S. (2012). Lumbar intervertebral disc degeneration associated with axial and radiating low back pain in ageing SPARC-null mice. *Pain*, *153*(6), 1167–1179. https://doi.org/10.1016/j.pain.2012.01.027

Millecamps, M., Tajerian, M., Sage, E. H., & Stone, L. S. (2011). Behavioral signs of chronic back pain in the SPARC-null mouse. *Spine*, *36*(2), 95–102. https://doi.org/10.1097/BRS.0b013e3181cd9d75

Mimura, M., Panjabi, M. M., Oxland, T. R., Crisco, J. J., Yamamoto, I., & Vasavada, A. (1994). Disc degeneration affects the multidirectional flexibility of the lumbar spine. *Spine*, *19*(12), 1371–1380. Retrieved from http://www.ncbi.nlm.nih.gov/pubmed/8066518

Miyagi, M., Millecamps, M., Danco, A. T., Ohtori, S., Takahashi, K., & Stone, L. S. (2014). ISSLS Prize winner: Increased innervation and sensory nervous system plasticity in a mouse model of low back pain due to intervertebral disc degeneration. *Spine*, *39*(17), 1345–1354. https://doi.org/10.1097/BRS.0000000000000334

Mohanty, S., Pinelli, R., Pricop, P., Albert, T. J., & Dahia, C. L. (2019). Chondrocyte-like nested cells in the aged intervertebral disc are late-stage nucleus pulposus cells. *Aging Cell*, *18*(5). https://doi.org/10.1111/acel.13006

Moore, K., Agur, A., & Dalley, A. (2015). *Essential Clinical Anatomy* (5th ed.). Wolters Kluwer.

Muriuki, M. G., Havey, R. M., Voronov, L. I., Carandang, G., Zindrick, M. R., Lorenz, M. A., … Patwardhan, A. G. (2016). Effects of motion segment level, Pfirrmann intervertebral disc degeneration grade and gender on lumbar spine kinematics. *Journal of Orthopaedic Research*, *34*(8), 1389–1398. https://doi.org/10.1002/jor.23232

Nachemson, A. (1960). Lumbar Intradiscal Pressure: Experimental Studies on Post-Mortem Material. *Acta Orthopaedica Scandinavica*, *31*(sup43), 1–104. https://doi.org/10.3109/ort.1960.31.suppl-43.01

Nilsen, N. J., Vladimer, G. I., Stenvik, J., Orning, M. P. A., Zeid-Kilani, M. V., Bugge, M., … Lien, E. (2015). A role for the adaptor proteins TRAM and TRIF in toll-like receptor 2 signaling. *Journal of Biological Chemistry*, *290*(6), 3209–3222. https://doi.org/10.1074/jbc.M114.593426

Niosi, C. A., & Oxland, T. R. (2004). Degenerative mechanics of the lumbar spine. *The Spine Journal*, *4*(6), S202–S208. https://doi.org/10.1016/J.SPINEE.2004.07.013

Nuckley, D. J., Kramer, P. A., Del Rosario, A., Fabro, N., Baran, S., & Ching, R. P. (2008). Intervertebral disc degeneration in a naturally occurring primate model: Radiographic and biomechanical evidence. *Journal of Orthopaedic Research*, *26*(9), 1283–1288. https://doi.org/10.1002/jor.20526

Nyati, K. K., Masuda, K., Mahabub-Uz Zaman, M., Dubey, P. K., Millrine, D., Chalise, J. P., … Kishimoto, T. (2017). TLR4-induced NF-κB and MAPK signaling regulate the IL-6 mRNA stabilizing protein Arid5a. *Nucleic Acids Research*, *45*(5), 2687–2703. https://doi.org/10.1093/nar/gkx064

O'Connell, G. D., Guerin, H. L., & Elliott, D. M. (2009). Theoretical and uniaxial experimental evaluation of human annulus fibrosus degeneration. *Journal of Biomechanical Engineering*, *131*(11). https://doi.org/10.1115/1.3212104

Pacifici M, Oshima O, Fisher LW, Young MF, Shapiro IM, L. P. (1990). Changes in osteonectin distribution and levels are associated with mineralization of the chicken tibial growth cartilage. - PubMed - NCBI. *Calcif Tissue Int.*, *47*(1), 51–61. Retrieved from https://www.ncbi.nlm.nih.gov/pubmed/2369692

Panjabi, M M. (1992). The stabilizing system of the spine. Part II. Neutral zone and instability hypothesis. *Journal of Spinal Disorders*, *5*(4), 390–396; discussion 397. Retrieved from http://www.ncbi.nlm.nih.gov/pubmed/1490035

Panjabi, Manohar M. (2003a). Clinical spinal instability and low back pain. *Journal of Electromyography and Kinesiology : Official Journal of the International Society of Electrophysiological Kinesiology*, *13*(4), 371–379. Retrieved from http://www.ncbi.nlm.nih.gov/pubmed/12832167

Panjabi, Manohar M. (2003b). Clinical spinal instability and low back pain. *Journal of Electromyography and Kinesiology : Official Journal of the International Society of Electrophysiological Kinesiology*, *13*(4), 371–379. Retrieved from http://www.ncbi.nlm.nih.gov/pubmed/12832167

Peck, S. H., McKee, K. K., Tobias, J. W., Malhotra, N. R., Harfe, B. D., & Smith, L. J. (2017). Whole Transcriptome Analysis of Notochord-Derived Cells during Embryonic Formation of the Nucleus Pulposus. *Scientific Reports*, *7*(1), 10504. https://doi.org/10.1038/s41598-

017-10692-5
Quero, L., Klawitter, M., Schmaus, A., Rothley, M., Sleeman, J., Tiaden, A. N., … Richards, P. J. (2013). Hyaluronic acid fragments enhance the inflammatory and catabolic response in human intervertebral disc cells through modulation of toll-like receptor 2 signalling pathways. *Arthritis Research & Therapy*, *15*(4), R94. https://doi.org/10.1186/ar4274
Raj, P. P. (2008). Intervertebral Disc: Anatomy-Physiology-Pathophysiology-Treatment. *Pain Practice*, *8*(1), 18–44. https://doi.org/10.1111/j.1533-2500.2007.00171.x
Rajan, N. E., Bloom, O., Maidhof, R., Stetson, N., Sherry, B., Levine, M., & Chahine, N. O. (2013). Toll-Like Receptor 4 (TLR4) Expression and Stimulation in a Model of Intervertebral Disc Inflammation and Degeneration. *Spine*, *38*(16), 1343–1351. https://doi.org/10.1097/BRS.0b013e31826b71f4
Roberts, S., Menage, J., & Urban, J. P. (1989). Biochemical and structural properties of the cartilage end-plate and its relation to the intervertebral disc. *Spine*, *14*(2), 166–174. Retrieved from http://www.ncbi.nlm.nih.gov/pubmed/2922637
Rodrigues, S. A., Wade, K. R., Thambyah, A., & Broom, N. D. (2012). Micromechanics of annulus–end plate integration in the intervertebral disc. *The Spine Journal*, *12*(2), 143–150. https://doi.org/10.1016/J.SPINEE.2012.01.003
Roughley, P. J., Melching, L. I., Heathfield, T. F., Pearce, R. H., & Mort, J. S. (2006). The structure and degradation of aggrecan in human intervertebral disc. *European Spine Journal*, *15*(S3), 326–332. https://doi.org/10.1007/s00586-006-0127-7
Rutges, J. P. H. J., Jagt van der, O. P., Oner, F. C., Verbout, A. J., Castelein, R. J. M., Kummer, J. A., … Dhert, W. J. A. (2011). Micro-CT quantification of subchondral endplate changes in intervertebral disc degeneration. *Osteoarthritis and Cartilage*, *19*(1), 89–95. https://doi.org/10.1016/J.JOCA.2010.09.010
Sage, E. H., & Bornstein, P. (1991). Extracellular proteins that modulate cell-matrix interactions. SPARC, tenascin, and thrombospondin. *The Journal of Biological Chemistry*, *266*(23), 14831–14834. Retrieved from http://www.ncbi.nlm.nih.gov/pubmed/1714444
Saravanakumar, K., & Harvey, A. (2008). Lumbar Zygapophyseal (Facet) Joint Pain. *Reviews in Pain*, *2*(1), 8–13. https://doi.org/10.1177/204946370800200103
Sarver, J. J., & Elliott, D. M. (2005). Mechanical differences between lumbar and tail discs in the mouse. *Journal of Orthopaedic Research*, *23*(1), 150–155. https://doi.org/10.1016/j.orthres.2004.04.010
Sato, K., Kikuchi, S., & Yonezawa, T. (1999). In vivo intradiscal pressure measurement in healthy individuals and in patients with ongoing back problems. *Spine*, *24*(23), 2468–2474. Retrieved from http://www.ncbi.nlm.nih.gov/pubmed/10626309
Schaefer, L. (2014). Complexity of danger: the diverse nature of damage-associated molecular patterns. *The Journal of Biological Chemistry*, *289*(51), 35237–35245. https://doi.org/10.1074/jbc.R114.619304
Sen, S., Jacobs, N. T., Boxberger, J. I., & Elliott, D. M. (2012). Human annulus fibrosus dynamic tensile modulus increases with degeneration. *Mechanics of Materials*, *44*, 93–98. https://doi.org/10.1016/j.mechmat.2011.07.016
Shinohara, H. (1999). The mouse vertebrae: changes in the morphology of mouse vertebrae exhibit specific patterns over limited numbers of vertebral levels. *Okajimas Folia Anatomica Japonica*, *76*(1), 17–31. Retrieved from http://www.ncbi.nlm.nih.gov/pubmed/10409842
Shirazi-Adl, A. (1992). Finite-element simulation of changes in the fluid content of human

lumbar discs. Mechanical and clinical implications. *Spine*, *17*(2), 206–212. Retrieved from http://www.ncbi.nlm.nih.gov/pubmed/1553592

Shirazi-Adl, A., Ahmed, A. M., & Shrivastava, S. C. (1986). A finite element study of a lumbar motion segment subjected to pure sagittal plane moments. *Journal of Biomechanics*, *19*(4), 331–350. https://doi.org/10.1016/0021-9290(86)90009-6

Smit, Theo H. (2002). The use of a quadruped as an in vivo model for the study of the spine – biomechanical considerations. *European Spine Journal*, *11*(2), 137–144. https://doi.org/10.1007/s005860100346

Smit, Theodoor H, van Tunen, M. S., van der Veen, A. J., Kingma, I., & van Dieën, J. H. (2011). Quantifying intervertebral disc mechanics: a new definition of the neutral zone. *BMC Musculoskeletal Disorders*, *12*, 38. https://doi.org/10.1186/1471-2474-12-38

Stokes, I. A. F., & Iatridis, J. C. (2004, December 1). Mechanical conditions that accelerate intervertebral disc degeneration: Overload versus immobilization. *Spine*. Spine (Phila Pa 1976). https://doi.org/10.1097/01.brs.0000146049.52152.da

Sweetwyne, M. T., Brekken, R. A., Workman, G., Bradshaw, A. D., Carbon, J., Siadak, A. W., … Sage, E. H. (2004). Functional Analysis of the Matricellular Protein SPARC with Novel Monoclonal Antibodies. *Journal of Histochemistry & Cytochemistry*, *52*(6), 723–733. https://doi.org/10.1369/jhc.3A6153.2004

Takashima, K., Matsunaga, N., Yoshimatsu, M., Hazeki, K., Kaisho, T., Uekata, M., … Ii, M. (2009). Analysis of binding site for the novel small-molecule TLR4 signal transduction inhibitor TAK-242 and its therapeutic effect on mouse sepsis model. *British Journal of Pharmacology*, *157*(7), 1250–1262. https://doi.org/10.1111/j.1476-5381.2009.00297.x

Takeda, K., Kaisho, T., & Akira, S. (2003). T OLL -L IKE R ECEPTORS. *Annual Review of Immunology*, *21*(1), 335–376. https://doi.org/10.1146/annurev.immunol.21.120601.141126

Termine, J. D., Kleinman, H. K., Whitson, S. W., Conn, K. M., McGarvey, M. L., & Martin, G. R. (1981). Osteonectin, a bone-specific protein linking mineral to collagen. *Cell*, *26*(1 Pt 1), 99–105. Retrieved from http://www.ncbi.nlm.nih.gov/pubmed/7034958

Urban, J. P. G., & Roberts, S. (2003). Degeneration of the intervertebral disc. *Arthritis Research & Therapy*, *5*(3), 120–130. Retrieved from http://www.ncbi.nlm.nih.gov/pubmed/12723977

Vaure, C., & Liu, Y. (2014, July 10). A comparative review of toll-like receptor 4 expression and functionality in different animal species. *Frontiers in Immunology*. Frontiers Research Foundation. https://doi.org/10.3389/fimmu.2014.00316

Vergroesen, P.-P.A., Kingma, I., Emanuel, K. S., Hoogendoorn, R. J. W., Welting, T. J., van Royen, B. J., … Smit, T. H. (2015). Mechanics and biology in intervertebral disc degeneration: a vicious circle. *Osteoarthritis and Cartilage*, *23*(7), 1057–1070. https://doi.org/10.1016/J.JOCA.2015.03.028

Vergroesen, Pieter-Paul A., van der Veen, A. J., van Royen, B. J., Kingma, I., & Smit, T. H. (2014). Intradiscal pressure depends on recent loading and correlates with disc height and compressive stiffness. *European Spine Journal*, *23*(11), 2359–2368. https://doi.org/10.1007/s00586-014-3450-4

Verstak, B., Stack, J., Ve, T., Mangan, M., Hjerrild, K., Jeon, J., … Mansell, A. (2014). The TLR signaling adaptor TRAM interacts with TRAF6 to mediate activation of the inflammatory response by TLR4. *Journal of Leukocyte Biology*, *96*(3), 427–436. https://doi.org/10.1189/jlb.2a0913-487r

Vincent, K., Mohanty, S., Pinelli, R., Bonavita, R., Pricop, P., Albert, T. J., & Dahia, C. L. (2019). Aging of mouse intervertebral disc and association with back pain. *Bone*, *123*, 246–

259. https://doi.org/10.1016/j.bone.2019.03.037

Vos, T., Allen, C., Arora, M., Barber, R. M., Bhutta, Z. A., Brown, A., … Murray, C. J. L. (2016). Global, regional, and national incidence, prevalence, and years lived with disability for 310 diseases and injuries, 1990–2015: a systematic analysis for the Global Burden of Disease Study 2015. *The Lancet*, *388*(10053), 1545–1602. https://doi.org/10.1016/S0140-6736(16)31678-6

Wang, Y., Videman, T., & Battié, M. C. (2012). Lumbar vertebral endplate lesions: prevalence, classification, and association with age. *Spine*, *37*(17), 1432–1439. https://doi.org/10.1097/BRS.0b013e31824dd20a

Woller, S. A., Ravula, S. B., Tucci, F. C., Beaton, G., Corr, M., Isseroff, R. R., … Yaksh, T. L. (2016). Systemic TAK-242 prevents intrathecal LPS evoked hyperalgesia in male, but not female mice and prevents delayed allodynia following intraplantar formalin in both male and female mice: The role of TLR4 in the evolution of a persistent pain state. *Brain, Behavior, and Immunity*, *56*, 271–280. https://doi.org/10.1016/J.BBI.2016.03.026

Yang, K. H., & King, A. I. (1984). Mechanism of facet load transmission as a hypothesis for low-back pain. *Spine*, *9*(6), 557–565. Retrieved from http://www.ncbi.nlm.nih.gov/pubmed/6238423

Yu, J., Peter, C., Roberts, S., & Urban, J. P. G. (2002). Elastic fibre organization in the intervertebral discs of the bovine tail. *Journal of Anatomy*, *201*(6), 465–475. https://doi.org/10.1046/j.1469-7580.2002.00111.x

Zhao, Y., Xin, Y., Gao, J., Teng, R.-Y., & Chu, H.-C. (2015). Analgesic effect of TAK-242 on neuropathic pain in rats. *International Journal of Clinical and Experimental Medicine*, *8*(7), 11202–11207. Retrieved from http://www.ncbi.nlm.nih.gov/pubmed/26379924

Zirbel, S. A., Stolworthy, D. K., Howell, L. L., & Bowden, A. E. (2013). Intervertebral disc degeneration alters lumbar spine segmental stiffness in all modes of loading under a compressive follower load. *The Spine Journal*, *13*(9), 1134–1147. https://doi.org/10.1016/j.spinee.2013.02.010